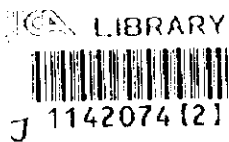


REPORT
ON
THE MINERAL EXPLORATION
IN
THE ESPIYE AREA,
THE REPUBLIC OF TURKEY

PHASE III

MARCH 1998



JAPAN INTERNATIONAL COOPERATION AGENCY
METAL MINING AGENCY OF JAPAN

MPN
JR
98-048

REPORT
ON
THE MINERAL EXPLORATION
IN
THE ESPIYE AREA,
THE REPUBLIC OF TURKEY

PHASE III

MARCH 1998

JAPAN INTERNATIONAL COOPERATION AGENCY
METAL MINING AGENCY OF JAPAN



1142074 [2]

P R E F A C E

The Government of Japan, in response to the request of the Government of Republic of Turkey, decided to conduct a mineral exploration composed of geophysical survey and drilling survey, in Espiye area, Republic of Turkey.


The Japanese Government entrusted the survey to the Japan International Cooperation Agency (JICA), and JICA in turn sought the cooperation of the Metal Mining Agency of Japan (MMAJ) to accomplish the survey, considering the importance of technical nature of the work.

The survey will be carried out within a period of three years commencing from 1995. The JICA and MMAJ dispatched the survey mission for phase III survey consisting of 5 members to Turkey from June 19th, 1997 to September 26th, 1997.

The field survey in Turkey was carried out successfully with cooperation of the Turkish Government authorities, and General Directorate of Mineral Research and Exploration. This report summarizes the result of the survey carried out in 1997 and also forms a part of the final consolidated report which will be submitted to the Government of Republic of Turkey after completion of the survey.

We wish to express our deep appreciation to the officials of the Government of Republic of Turkey and to the Embassy of Japan in Turkey concerned for their close cooperation extended to the survey mission.

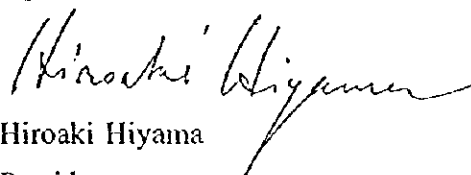
March, 1998



Kimio Fujita

President

Japan International Cooperation Agency



Hiroaki Hiyama

President

Metal Mining Agency of Japan

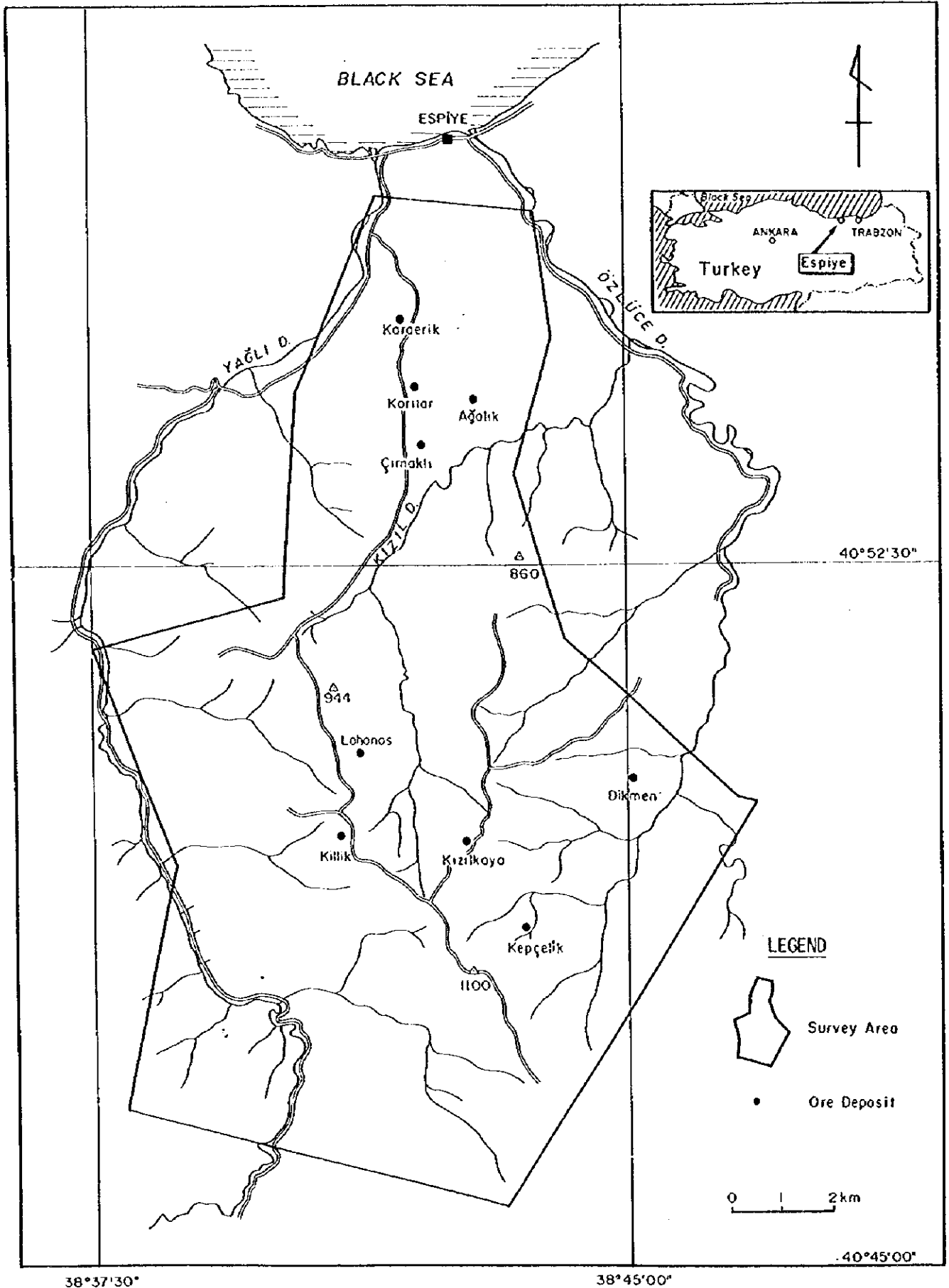


Fig.I-1 Location Map of the Survey Area

Summary

This survey was carried out in order to study the geological frame work and discover new ore deposits of massive sulfide type in the Espiye area, the Republic of Turkey. At the same time, technological transfer from Japan to the related organization of Turkey is one of the purpose of this project.

The survey of this year (phase III) includes the geophysical survey (IP method and CSAMT method) and 2 holes of drilling survey (total 750m) in Karılar area where is located in northern part, selected as a promising area in the Phase I survey, and 2 holes of drilling survey (total 500m) in Taflancık area where there is high potential of existence of ore deposit.

Cu-Zn veins (MJTE-9) related to the massive ore body and a strong argillized zone (MJTE-10) accompanied by a stockwork of pyrites in footwall dacite were confirmed in Taflancık area, but no massive ore body was discovered. Judging from the survey results so far obtained, the alteration and mineralization in footwall dacite and the distribution of wide IP anomaly zone indicated that there was a strong hydrothermal activity. It is highly possible that a massive ore deposit was formed in this area. However, since a development of horizon tuff was not observed, the ore body might had been eroded out already.

As the results of the geophysical survey (IP), 2 anomaly zones reflecting well the old mines, were observed in Karılar area, and it turned out that of these anomalies were accompanied by a weak anomaly in the depth. Geologically, since it was thought that the ore horizon corresponds to this weak anomaly zone, the existence of ore body was expected. As the results of the drilling survey, however, only a weak pyritic stockwork was confirmed in the depths of MJTE-12. It turned out that the ore horizon becomes deeper toward the north (MJTE-11) and the old ore deposits do not indicate a massive type mineralization but these might be formed by a newer stockwork type mineralization.

Based on the above-mentioned facts and the three years survey results, we propose the following for the future survey and study.

1. Although the exploration of promising areas has been almost completed, it is advisable to conduct the IP survey at a great exploration depth and the drilling survey in Çalkaya area where no drilling survey has been carried out yet.
2. To conduct the detailed survey on footwall dacite to clarify a relation with the massive sulfide ore deposit.
3. To re-examine the ore showings of the massive sulfide ore deposits in a metallogenic province of massive sulfide along the coast of the Eastern Black Sea.



	Pages
1-1 IP Survey	21
1-2 CSAMT Survey	59
1-3 Consideration	70
Chapter 2 Drilling Survey	75
2-1 Survey Method	75
2-2 Results of the Survey	77
2-3 Consideration	83
PART III Conclusion and Recommendation	101
Chapter 1 Conclusion	101
Chapter 2 Recommendation in the Future Projects	102
References	105

Appendices

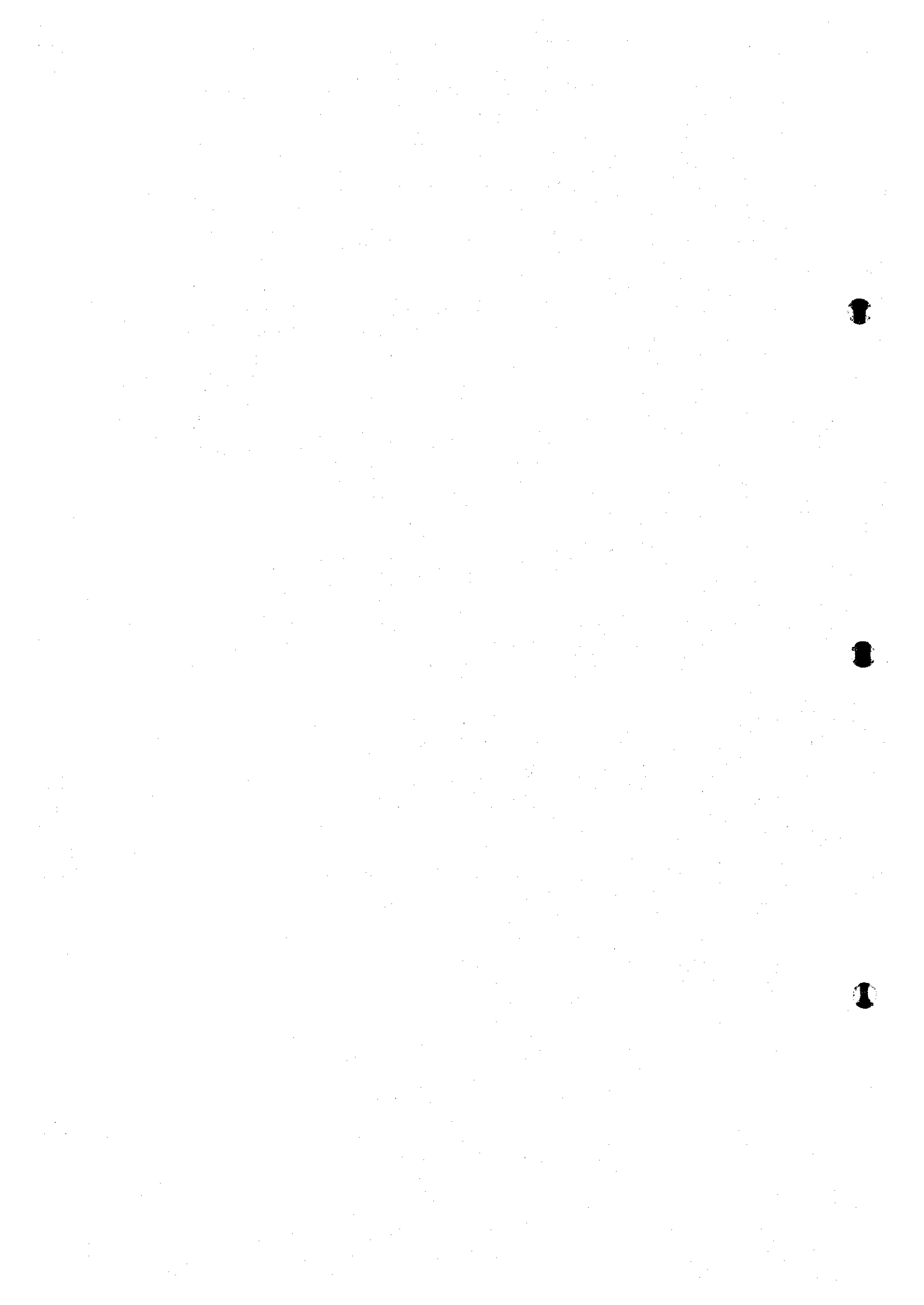
Figures

Fig.I-3-1 Metallogenic Province of East Black Sea Region	11
Fig.I-4-1 Geological Map	15
Fig.I-4-2 Schematic Lithostratigraphy	17
Fig.II-1-1 Location of the Geophysical Survey Area	22
Fig.II-1-2 Location of the IP Survey Lines and CSAMT	23
Fig.II-1-3 Concept of IP Operation	25
Fig.II-1-4 Concept of the IP Method of Measurement	25
Fig.II-1-5 IP Section of Apparent Resistivity and Chargeability (Line A)	29
Fig.II-1-6 IP Section of Apparent Resistivity and Chargeability (Line B)	30
Fig.II-1-7 IP Section of Apparent Resistivity and Chargeability (Line C)	31
Fig.II-1-8 IP Section of Apparent Resistivity and Chargeability (Line D)	32
Fig.II-1-9 IP Section of Apparent Resistivity and Chargeability (Line E)	33
Fig.II-1-10 IP Section of Apparent Resistivity and Chargeability (Line F)	34
Fig.II-1-11 IP Section of Apparent Resistivity and Chargeability (Line G)	35
Fig.II-1-12 IP Plane Map of Apparent Resistivity	36
Fig.II-1-13 IP Plane Map of Apparent Chargeability	37

	Pages
Fig.II-1-14 Relation between Apparent Resistivity and Chargeability of Rock and Ore Samples	45
Fig.II-1-15 MF Property of Rock and Ore Samples	45
Fig.II-1-16 IP Section of Simulated Result (Resistivity)	47
Fig.II-1-17 IP Section of Simulated Result (Chargeability)	49
Fig.II-1-18 IP Plane Map of Simulated Result (Resistivity)	51
Fig.II-1-19 IP Plane Map of Simulated Result (Chargeability)	52
Fig.II-1-20 IP Section of Simulated Result (M F)	53
Fig.II-1-21 IP Plane Map of Simulated Result (M F)	55
Fig.II-1-22 IP D Section of Simulated Result (a=100m)	56
Fig.II-1-23 IP E Section of Simulated Result (a=100m)	57
Fig.II-1-24 Measurement Concept of the CSAMT Survey	60
Fig.II-1-25 CSAMT Section of Apparent Resistivity	64
Fig.II-1-26 CSAMT Plane Map of Apparent Resistivity	65
Fig.II-1-27 CSAMT 1-D Resistivity Structure column	66
Fig.II-1-28 CSAMT 1-D Section of Resistivity Structure	67
Fig.II-1-29 CSAMT 1-D Plane Map of Resistivity Structure	68
Fig.II-1-30 CSAMT 2-D Map of Resistivity Structure	69
Fig.II-1-31 Summarized Map of Geophysical Survey	73
Fig.II-2-1 Location of the Drilling Survey Area	85
Fig.II-2-2 Location of the Drilling Sites	86
Fig.II-2-3 Geological Columnar Section of MJTE-9 (Appendices)	A-1
Fig.II-2-4 Geological Columnar Section of MJTE-10 (Appendices)	A-4
Fig.II-2-5 Geological Columnar Section of MJTE-11 (Appendices)	A-7
Fig.II-2-6 Geological Columnar Section of MJTE-12 (Appendices)	A-11
Fig.II-2-7 Geological Section (Taflancık Area)	97
Fig.II-2-8 Geological Section (Karılar Area)	99
Tables	
Table I-1-1 List of Survey Amount	5
Table II-1-1 Specifications of the IP Survey	21
Table II-1-2 List of Sampling Time	25
Table II-1-3 List of IP Equipment and Materials	26
Table II-1-4 Results of IP Survey	38
Table II-1-5 Results of Physical Property Tests	44

	Pages
Table II-1-6 Summarized Table of IP Survey	58
Table II-1-7 CSAMT Survey Method	59
Table II-1-8 List of CSAMT Equipment and Materials	60
Table II-2-1 List of Main Drilling Equipment	87
Table II-2-2 List of Drilling Equipment and Consumption Goods	88
Table II-2-3 List of Used Diamond Bits and Reaming Shells	88
Table II-2-4 Drilling Summary (MJTE-9)	89
Table II-2-5 Drilling Summary (MJTE-10)	90
Table II-2-6 Drilling Summary (MJTE-11)	91
Table II-2-7 Drilling Summary (MJTE-12)	92
Table II-2-8 Drilling Schedule	93
Table II-2-9 Results of Chemical Analysis	94
Table II-2-10 Results of X-Ray Diffraction Analysis	95
Table II-2-11 Results of Microscopic Observation of Thin Section	96
Table II-2-12 Results of Microscopic Observation of Polished Section	96

PART I General Remarks



PART I General Remarks

Chapter 1 Introduction

1-1 Background and Purpose

This survey will be held for three years from 1995, and this year is the third year in this survey. The survey area was established around Espiye area in the Republic of Turkey where massive sulfide ore deposits can be highly expected to exist. It is urgently important to explore in this area and to evaluate, because real exploration works have not been carried out sufficiently.

Then the government of Turkey requested Japanese government to survey for mineral resources in the above-mentioned area, under joint technological cooperation with Japanese side. The government of Japan, in response to the request from the government of Turkey, decided to conduct the basic survey such as geophysical survey and drilling survey for discovery of new ore deposits, and to transfer the technology to Turkish side, as third year's program.

1-2 Conclusion and Proposal of the Second Year's Survey

1-2-1 Conclusion of the Second Year's Survey

We executed a geophysical survey (IP method, the total extension of the survey line is 30km) and investigated eight boreholes (the total drilling length is 1749m) in a promising area selected in the first phase and this phase of the survey. The following is a summary of the survey results in each area.

1. Bitene area (Three boreholes for survey)

The holes were drilled in the north-east to north north-east of the Killik ore deposit at MJTE-3 and 4. For the geological point of view, it was clarified that tuffs of the Çağlayan Formation developed relatively thickly on a gentle slope over footwall dacite. The appearance depth of the footwall is 710 to 730m above sea level and it is higher than the altitude (about 650 m) of the Lahanos ore deposit. The ore horizon gently inclines toward the north.

As for mineralization, a predominant stockwork zone was captured in the footwall dacite at MJTE-3 and a yellow ore part (Cu=12.58%, Au=2.06ppm) was observed at 20cm from the upper part.

MJTE-5 was drilled at a position 200 to 300m south of the end of the Lahanos ore deposit. It was clarified that relatively thick aphyric dacite of the Çağlayan Formation was observed from the surface and tuffs were not distributed. The footwall dacite appears at 650m above sea level and this is almost equal to the depth of the ore horizon in the Lahanos ore deposit. A development of a slightly predominant networked powder pyrite is observed in the footwall dacite, but the ore grade is low. However, it turned out that there were veinlets of

copper and zinc and the alteration accompanied mainly by sericite and kaoline occurred on the hanging wall Çağlayan Formation.

The Bitene area is located between the Lahanos ore deposit and the Killik ore deposit, and an existence of a new ore deposit was expected. But, the relatively predominant mineralization of footwall was only observed. Since there is little room for exploration because an intrusive rock body is distributed in the middle, it is thought that the probability of an existence of a large-scale strata-bound massive sulfide ore deposit is low.

2. Killik area (Three IP survey lines, one borehole for drilling survey)

The geophysical survey (IP method) revealed that a strong anomaly zone existed in the southern part of the area, south from the south-east slope of the Yeniyolbaşı Mountain.

However, a strata-bound ore deposit cannot be expected because the anomaly part is in the distribution area of the footwall dacite, but the possibility still remains that a network-vein type large-scale low grade ore deposit (Murgul type) exists. A further survey will clarify the details.

The drilling survey (MJTE-1) was carried out at a point between the Killik ore deposit and the Kızılkaya ore deposit where the hanging wall was distributed and the above-mentioned IP anomaly continued into the depths. From top to down, thick hematite dacite, thin dacite lava of Çağlayan Formation and the footwall dacite of Kızılkaya Formation were observed, but tuffs of the Çağlayan Formation were not observed.

Both alteration and mineralization were found on and below the Çağlayan Formation and a 25cm thick dissemination zone (Cu=4.88%) of chalcopyrite was observed in the footwall dacite. Comparing a mineralization through the drilling with the IP results, the exploration depth of the IP method in this part is about 200m.

As mentioned above, there is a possibility of an existence of a Murgul-type ore deposit in this area. Considering the IP surveys (phase I and II survey), a small-scale strata-bound type ore body may exist directly below the ridge in the southern part of the Yeniyolbaşı Mountain.

3. Keçelik area (Two IP survey lines, one borehole for drilling survey)

In the geophysical survey (IP method) we observed a weak anomaly in the depths in the southwestern part of the survey lines, and we conducted a drilling survey (MJTE-2) for this anomaly. The survey revealed a dissemination-type and vein-type weak mineralization and clarified that the Kızılkaya Formation dacite was very thin. It was judged that the probability of an existence of a large-scale ore deposit was low.

4. Taflancık area (Four IP survey lines, three boreholes for drilling survey)

This area was an unexploited area. With the help of the anomaly obtained from the results of the IP survey of the phase I, we carried out an IP survey in second year and successfully found a new anomaly zone.

The plane distribution direction of the anomaly zone indicates NNE-SSW and corresponds with the distribution direction of the Lahanos ore body. In the Taflancık area, a distribution of two anomaly zones (northwest and southeast) in echelon form has been defined in plane map of apparent chargeability ($n=3-4$). MJTE-6 is located near northwest anomaly zone, MJTE-8 is located in end of southeast anomaly zone and MJTE-7 is located near center of southeast anomaly zone.

Geologically, this area is composed of hematite dacite, dacite lava of Çağlayan Formation, dacitic lava and tuff of Kızılkaya Formation and those units show a gentle north dip.

It presents the alteration mainly accompanied by sericite and kaolinite at MJTE-7 and chlorite shows a tendency to be predominant toward the north.

The mineralization of pyrite dissemination-network and a small amount of disseminated chalcopyrite are observed, which is the strongest in the footwall dacite at MJTE-7 and extends to the shallowest part at MJTE-8.

Microscopic investigation showed that the mineralization was accompanied by a trace of sphalerite and colloform and framboidal pyrite.

Since yellow ore fragments were obtained in MJTE-6, it was presumed that a supply source existed nearby. Although strong mineralizations have been observed in MJTE-7 and MJTE-8, massive ore body could not be discovered. The source area for yellow ore fragments is supposed to be in the northwest IP anomaly zone.

Judging from the above-mentioned facts, the probability of an existence of a massive sulfide ore deposit is high in this area so that we hope for a drilling survey to the northwest IP anomaly zone in the future.

5. Çalkaya area (Five IP survey lines)

Only a continuous weak IP anomaly was partly observed from a weakly mineralized outcrop and a new anomaly zone could not be obtained. It may be partly because the hanging wall is thick, but at the present time we cannot help judging that the probability of existence of ore deposit is low in this area.

6. Other areas

The Karaerik-Çımaklı area is one of selected promising areas in the first phase of the survey. It is clear that the previous surveys have not reached the massive ore horizon. Judging from the alteration accompanied mainly by sericite and kaolinite and a geochemical anomaly, the possibility of existence of ore deposit still remains in the further depths (200 to 350m).

7. The age determination of sericite in the alteration zone clarified that the age of the alteration related to the Kızılkaya and Karaerik ore deposits is 77Ma.

1-2-2 Proposal to the Third Year's Program

Based on the results obtained from the second phase of the survey, we suggest that the third phase of the survey be conducted in the following areas. We describe those areas in order of priority.

1. Taflancık area

Since an ore deposit may exist in a new anomaly zone extending in the same direction as that of the Lahanos that obtained by the geophysical survey IP method, the drilling survey should be conducted in the third phase of the survey.

2. Karaerik-Çımaklı area

This is an area where ore showings exist on the surface and the potential of an existence of an ore deposit is high. Sufficient exploration has not been carried out so far. Therefore, it is advisable to apply the geophysical survey IP and CSAMT methods and to conduct the drilling survey in promising area.

3. Killik area

A strata-bound type ore deposit is less expected in a strong anomaly zone which distributed from the southeastern slope of the Yeni Yolbaşı Mountain to the south defined by the geophysical survey IP method, but the possibility of a large-scale network-vein type low grade ore deposit (Murgul type) still remains. It is recommended that an IP survey be conducted along E-W trending valley and ridge of the south end to define an extension of the mineralization and a drilling survey be carried out in a promising area.

Also, results of the IP survey revealed a possibility that an ore body might exist in the south ridge of the Yeni Yolbaşı Mountain. In order to verify this, it is desirable that a drilling survey be conducted.

1-3 Outline of the Third Year's Survey

1-3-1 Survey Area

Taflancık and Karılar Area were selected for Phase III Survey. Because massive sulfide deposit of Lahanos type has been expected on Taflancık by geophysical and drilling survey in Second Year. And In spite of high potential of mineralization in Karılar Area, there exist not enough exploration.

1-3-2 Purpose of the Survey

The main purpose of the survey in Taflancık Area was to obtain the state of mineralization and to evaluate the potential by drilling survey. The purpose of geophysical and drilling survey in Karılar Area was to clarify geological structure, mineralization and the continuity of ore horizon.

1-3-3 Method and Content of the Survey

Geophysical survey (IP Method, CSAMT Method), drilling survey and laboratory test were carried out. The content of these survey were summarized below in Table I-1-1.

Table I-1-1(1) List of Survey Amount (drilling)

Drilling No.	Depth(m)	Inclination	Area
MJTE-9	250	-90 °	Taflancık
MJTE-10	250	-90 °	Taflancık
MJTE-11	400	-90 °	Karılar
MJTE-12	350	-90 °	Karılar
TOTAL	1,250		

Table I-1-1(2) List of Survey Amount (Geophysical Survey and Laboratory Test)

Items		Amount
Geophysical Survey	IP Method	7lines total 21.4Km (a=200m,a=100m)
	CSAMT Method	25 points
Laboratory Test	Thin Section	12
	Polished Section	10
	X-Ray diffraction	33
	Chemical Analysis (Cu,Pb,Zn,Au,Ag,Fe,S)	31
	Measurement of resistivity and chargeability	23

1-3-4 Survey Team

Members Participating in this survey are as follows.

Survey Team

Japanese Members			Turkish Members		
Shigehisa FUJIWARA	Leader	Dowa	Nevzat KARABALIK	Project Manager	MTA*
Tatuhiko AOYAMA	Drilling	"	Huseyin YILMAZ	Camp Leader	"
Kuraei IWAKI	Geophysist	"	Mustafa K:KURUÇELİK	Geologist	"
Norikiyo SUGIURA	"	"	Ali FaiK ALTINBAŞ	"	"
Masatoshi MAEKAWA	"	"	Turgut ÇOLAK	"	"
			Ömer DUMAN	Geophysist	"
			Kadir DEMİR	"	"
			Mustafa DEMİRHAN	"	"
			Hurşit ASLANOĞLU	Drilling	"
			Avni AKDENİZ	"	"
			Etem OFLU	Measurement	"

*:MTA (General Directorate of Mineral Research and Exploration)

Supervisor in Turkey

Tadashi ITO MMAJ (Metal Mining Agency of Japan)

Eishi ENDO "

1-3-5 Terms of the survey

Field survey was carried out as follows.

Survey in Turkey : 1997 / Jun / 19 ~ 1997 / Sep / 26

Geophysical Survey : 1997 / Jun / 19 ~ 1997 / Aug / 8

Drilling Survey : 1997 / Jun / 19 ~ 1997 / Sep / 26

Chapter 2 Geography in the Survey Area

2-1 Location and Transportation

The Espiye area is an area of 150km² extending south from Espiye Town (population of about 10,000) located about 100km west of Trabzon City, a major city along the coast of the Black Sea, in the north-east area of the Republic of Turkey (Fig.I-1). It takes about one hour from Ankara, the capital, to Trabzon by air and less than two hours are required by car from Trabzon to Espiye through a paved road along the Black Sea.

This region belongs to Giresun Prefecture of which center is Giresun City located 30km west of Espiye Town in terms of administrative division.

The survey area is a hazelnut-producing area and is dotted with small villages. An unpaved road in bad condition leads to each village. However, they are often closed to traffic during the rainy season. It takes about one and half hours by car with four-wheel drive from Espiye Town, a base town, to Taflanlık, the southern end of this year's survey area.

2-2 Topography and Drainage

Within this survey area belonging to the Black Sea coast part, a fold mountain range (Inoue, 1970) formed in the beginning of the Alpine orogenic cycle, called as the East Black Sea Mountain Range falls sharply into the vicinity of the coast, and there is little flat land. For this reason, the area is tens of meters to about 1,500meters high above the sea level and its land form is steep and relatively rich in undulations.

The survey area is divided into two by a dividing ridge running from north to south in the center. That is, the eastern part belongs to the upper reaches of the river system of Kızıl Dere and Karadona Dere, a branches of Özlüce Dere. The western part corresponds to the upper reaches of branch streams of the Yağlı Dere system. These streams form a steep V-shaped valley.

2-3 Climate and Vegetation

This area which has the heaviest rainfall and snow in the Republic of Turkey belongs to a Black Sea type climate (MMAJ, 1970) because a warm and wet wind from the Black Sea blows against the Black Sea Mountains. For this reason, the vegetation grows thick. Rainfall is plentiful from September through March and the average rainfall for October in Trabzon reaches 300 mm. In November rain turns to snow. The average temperature in August reaches the maximum, 24 °C, and that in February falls to the minimum, 6 °C.

Since this area is a hazelnut-producing area, even a steep mountainous slopes are covered with these trees in many places. Particularly, this tendency is significant in the northern part. Natural plants can be often seen in high elevation area of the southern part and shrubs such as

rhododendrons grow thick with some evergreen oak trees and beech trees.

Chapter 3 General Geology

3-1 Outline of Geology

Turkey is geologically divided into three areas of Pontides in the north, Anatolides in the middle, and Taurides in the south (Kormaz et al. 1992). The survey area is located in the north-east of the Pontides area. The basement in the Pontides area consists of metamorphic rocks and granitic rocks, and six stratigraphical units are distributed over it. They are Paleozoic, early Jurassic system-early Cretaceous system, late Cretaceous system-early Paleocene series, middle Paleocene-late Eocene series, Miocene series-Pliocene, and Pliocene series-Quaternary system in this order from the lowest layer.

Volcanic rocks belonging to the late Cretaceous system-early Paleocene are continuously distributed along the coast of the east Black Sea including this area and they are accompanied by massive sulfide type mine represented by Murgul, Çayeli, Lahanos, etc..

Güven et al (1992) classified the late Cretaceous system-early Paleocene into the Çatak formation mainly composed of andesitic-basaltic volcanics, Kızılkaya formation mainly composed of dacitic volcanics, and Çağlayan formation composed of andesite-basaltic lava, pyroclastics, and part of dacitic volcanics from the lowest layer. In addition, an intermittent distribution of granitic rocks which are thought to belong to the Tertiary period is observed in this zone.

From a structural point of view, the area along the coast of the Eastern Black Sea including this area is located in the north of the northern Anatoria Fault (WNW-ESE) which is a right-lateral transform fault and is classified as a Pontides orogenic zone as mentioned above.

It is thought that a deep fracture of an E-W~NE trending is related to the magmatism after Cretaceous period along the coast of the eastern Black Sea (Çagatay, 1993).

3-2 Mineralization and Mineralization Zone

The eastern Black Sea area is a major metallogenic province in the Republic of Turkey (see Fig.I-3-1) and is accompanied by many ore deposits of copper, lead, zinc, iron sulfide, gypsum, etc. Among others, it is said that this area produces about 70% of the domestic yield of copper.

Various types of ore deposits are known in this metallogenic province. As a general tendency, a zonal arrangement is observed in order of porphyry Cu type, skarn deposit, network - vein copper/iron sulfide deposit, massive-lenticular iron/copper/lead/zinc sulfide ore deposit, and manganese-hematite ore deposit from the mountain ridge toward the coast of the Black Sea. Among these, it is thought that a zone of the massive-lenticular iron/copper/lead/zinc sulfide ore deposits crosses the boarder into Georgia.

Among these ore deposits, a massive sulfide ore deposit is particularly important. Murgul and Çayeli, a typical ore deposit, have the following features. Both ore deposits are formed in dacite lava of upper part of Kızılkaya formation and the ore deposits are covered with relatively thick hematite dacite through a thin tuff of the hanging wall in Murgul. The ore deposit in Çayeli is covered with tuff and basaltic lava.

Ores in Murgul have the characteristic of stringer and dissemination. The aggregate of veinlets containing copper is the subject of the open-cut mining. Zinc and gypsum exist only in the upper part of an ore body. An ore body in Çayeli is a steep lenticular form, and elastic ores rich in sphalerite, massive black ore, and yellow ore are found in this order from the top. Ores in the Lahanos ore deposit existing in the survey area resemble Çayeli ores, except that the distribution form of the Lahanos ore deposit is almost horizontal.

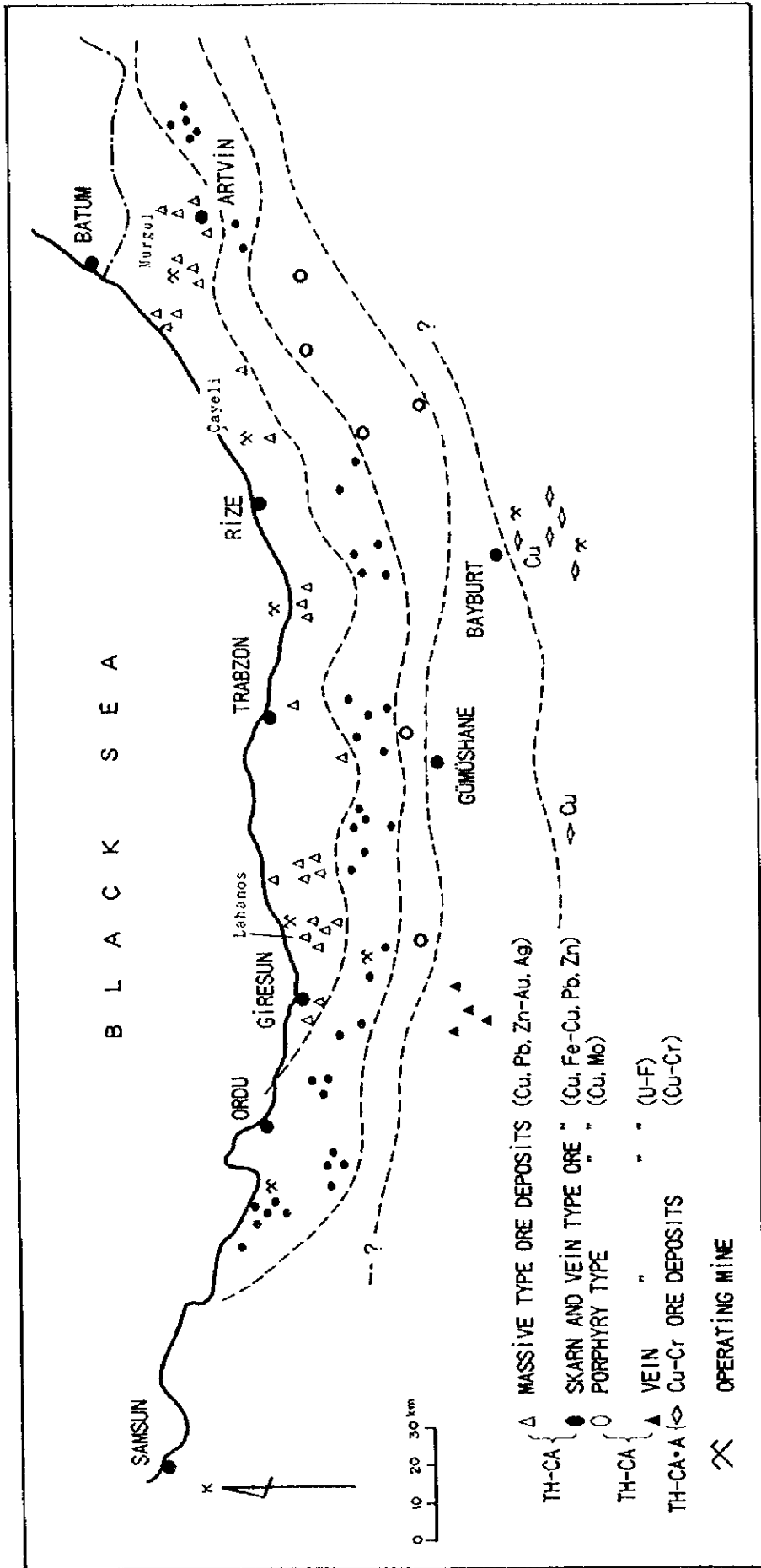


Fig.1-3-1 Metallogenic Province of East Black Sea Region

Chapter 4 General Discussion on Survey Results

4-1 Geological Structure, Characteristics of Mineralization, and Mineralization Restrictions

The survey area geologically consists of, from the lower layer, the Çatak Formation mainly containing andesitic volcanics, the Kızılkaya Formation mainly containing dacitic lava accompanied by dacitic pyroclastics, and the Çağlayan Formation mainly composed of dacitic-rhyolitic volcanics accompanied by a lot of intrusive rocks. The geological map and schematic lithostratigraphy are shown in Fig. I-4-1~Fig.I-4-2.

The massive sulfide ore deposits along the coast of the Black Sea including this area is similar to the kuroko type ore deposits in Japan, accompanied by a lot of acidic volcanics, and bound by strata. Since the Lahanos deposit which is in operation in this area, is hosted in top of the Kızılkaya Formation, the survey is carried forward with focusing the promising area, taking into consideration the alteration and geophysical survey results in the distribution area of the Çağlayan Formation covering the Kızılkaya Formation.

The distribution of ore showings and ore deposits concentrated in the northern part (Karaerik-Çımaklı) and the central part (Lahanos-Taflancık). In the northern part, the Karaerik and Karılar deposits except the Ağalık deposit are considered to have a stockwork type mineralization newer than the Lahanos massive ore deposit, and distributed in a direction of ENE-WSW. In the central part including the Lahanos and Kızılkaya deposits, the mineralization zone composed of massive ore deposits and network zones of its footwall continues in the NE-SW direction with a width of at least 3km or more. In particular, the continuity of this zone has been traced to northeastward cross the area. Furthermore, a group of massive sulfide ore deposits are scattered in the south from Tirebol, 20km northeast from Espiye. Judging from this, it can be said that there is a strong possibility that the massive sulfide ore deposits were formed by being restricted by the NE-SW system structure around this region.

4-2 Relationship between Geophysical Survey Results and Mineralization

The IP survey has been conducted for two consecutive years in Phase I and Phase II. It turned out that the IP anomalies reflected the mineralization in footwall dacite well. The IP survey of this year was conducted with a greater exploration depth (at longer measurement point intervals).

The analytical results along survey lines, old mines reflected the concept of the mineralization well. That is, in the Karaerik deposit a lenticular anomaly was observed in a relatively shallow part and it is thought that this lenticular part used to be a target for mining. According to the results of MJTE-11, the mineralized part corresponds to the dacitic volcanic rock distribution zone in a shallow part, and there is a possibility that the ore forming fluid rose

from the south along the upper contact of the dacite intrusive located below that. It was expected that a weak anomaly analyzed in the depths of MJTE-11 was caused by a massive type mineralization, but it turned out that this anomaly was chiefly due to montmorillonite content etc. in this unit.

A steep IP anomaly zone was defined in the Karılar deposit, indicating well that this deposit was not of strata-bound type as used to be considered before this project but was a network- vein type ore deposit. Unlike the one found in a shallow part, the IP anomaly in the deep part seemed to be distributed in a wide and indicated the existence of the massive sulfide ore deposit. Since the MJTE-12 drilling survey results revealed that the IP in the deep level reflected the development of a stockwork of pyrite as in a shallow part, it is thought that the higher IP values must be measured if a large-scale massive ore body exists. Also, according to the CSAMT survey executed simultaneously, an EW or ENE trending structure passing near the Karılar and Karaerik deposits was found. This structure might be related to the mineralization of these deposits.

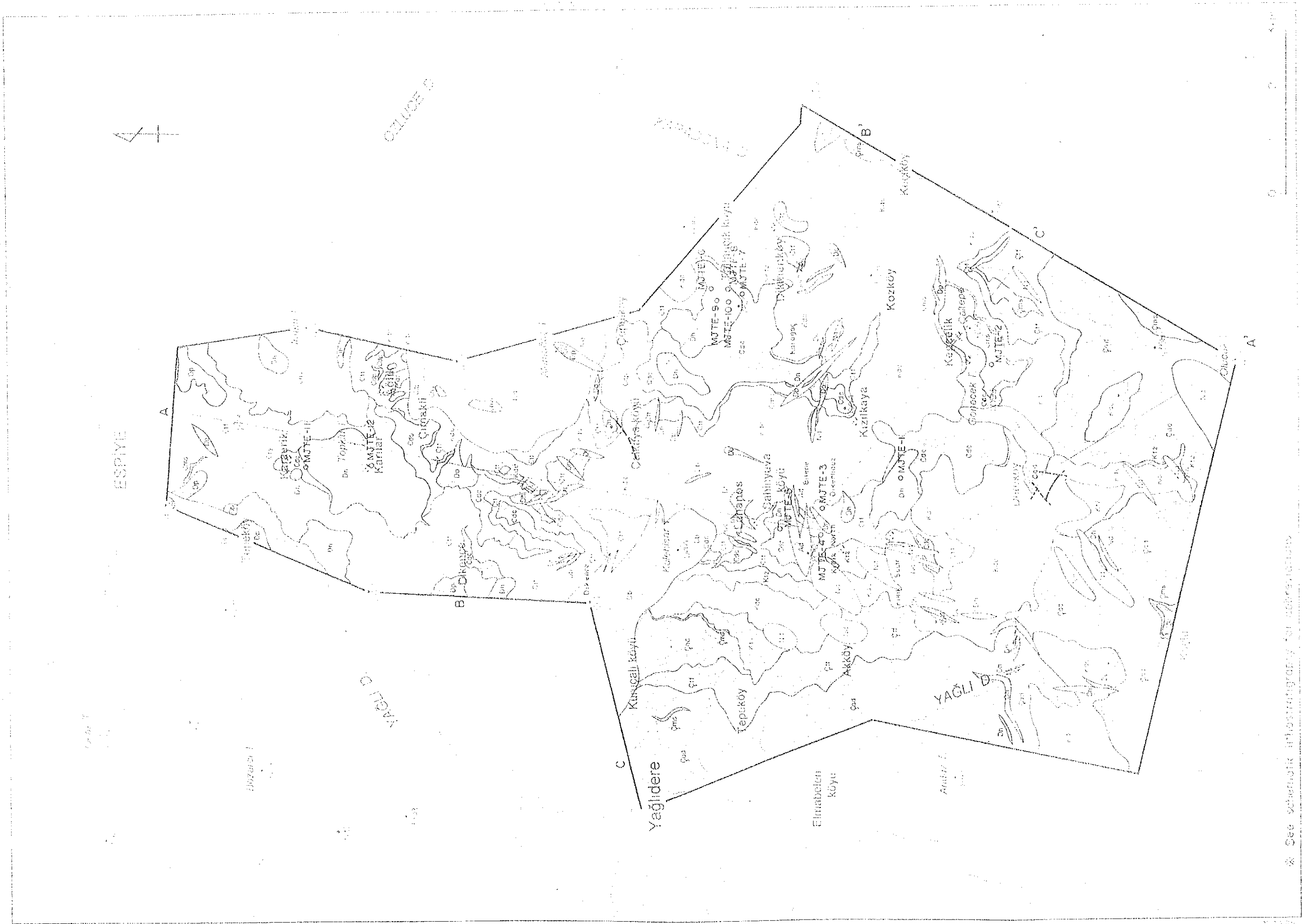
4-3 Potentiality of Expectancy of Ore Deposit

The survey area occupies a part of the eastern Black Sea Metallogenic Province which is the most important copper producing district in the Republic of Turkey. Since this area has many massive sulfide ore deposits and ore showings such as, the Lahanos mine, it was expected to discover new ore deposits.

A full-scale survey has not been carried out in the Taflancık area prior to this survey. As the results of five drilling surveys conducted in Taflancık area, a predominant stockwork zone was confirmed in footwall dacite and fragments of high grade yellow ore were captured near the ore horizon, but the massive ore body was not discovered. The ore body might have eroded out and it was judged that there was little possibility of a existence of a large-scale ore body near the Taflancık area.

In the Karılar area, the Karaerik and Karılar deposits are thought to be a kind of new hydrothermal ore deposits, although they have been treated as the massive type mineralization before this project. Geologically, It is made clear that the Karılar area is covered with the thick volcanic rocks of the Çağlayan Formation. As the IP survey revealed that no strong IP anomaly indicated there was little possibility to find new ore body in the depths of 300 to 400m below the surface of the earth, it is assumed that a massive ore deposit might be exist in a deeper part if any.





* See schematic lithostratigraphy for abbreviations.

Fig.1-4-1 Geological Map

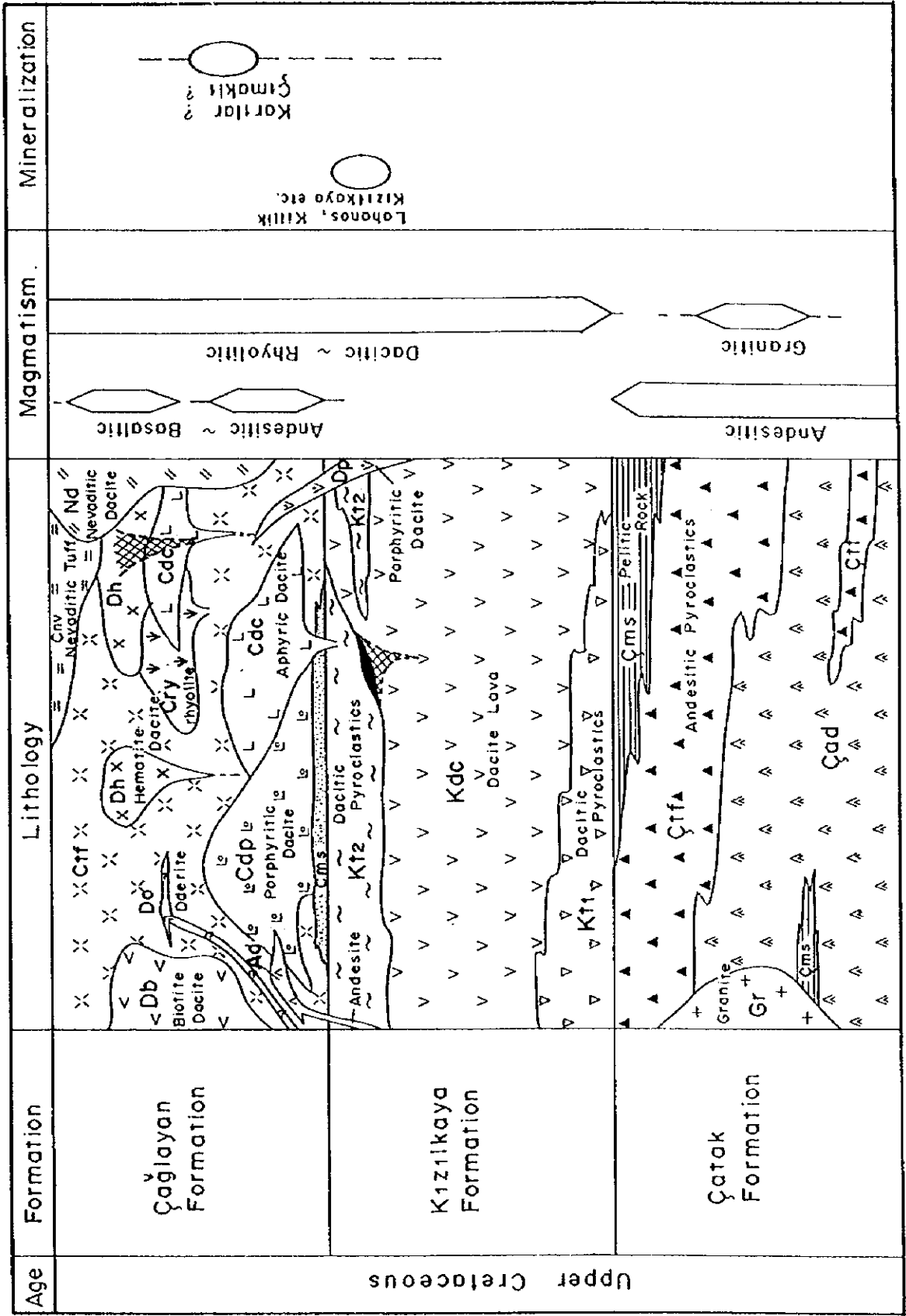


Fig.1-4-2 Schematic Lithostratigraphy

Chapter 5 Conclusion and Recommendation

5-1 Conclusion

The drilling survey of two boreholes (total 500m) in the Taflancık area and the geophysical survey (IP and CSAMT methods) and the drilling survey of two boreholes (total 750m) in the Karılar area were conducted in this year. The survey results in each area were summarized as shown below.

1. Taflancık area

Last year the drilling of three boreholes was carried out in the eastern part of the anomaly zone defined by IP survey, where yellow ore fragments, a network zone in a footwall, and an alteration zone were confirmed. The exploration of MJTE-9 and MJTE-10 was carried out in this year for the purpose of prospecting the northwestern area of this anomaly zone.

MJTE-9 is located in the northern part of the anomaly zone, at a point 300m away from MJTE-6 to the southwest. Its geology can be correlated to MJTE-6 and the dip of strata is almost horizontal between these two points. MJTE-9 is accompanied by veinlets of Cu-Pb-Zn in the depths but the mineralization is weak on the whole. The alteration is also weak compare to other holes and there are not so many fragments of mineralized and altered rocks which are found in a large quantity at MJTE-6. Judging from these survey results, it is concluded that MJTE-9 is located far from the back ground zone of altered fragments etc. compared to MJTE-6.

MJTE-10 is located in the middle western part of the anomaly zone. It indicates almost the same geology and mineralization as MJTE-8. That is, the mineralization mainly containing pyrites was found on the whole Kızılkaya Formation, but the chemical analysis revealed that each element showed low value and no development of horizon tuff was found. Judging from these survey results, it is highly possible that the ore body might have been eroded out in this area although it would have formed before.

2. Karılar area

Some old mines such as Karaerik, Karılar, and Çımaklı are known in this area. Those were generally believed to be the strata-bound type massive sulfide deposits. But, the survey in Phase I suggested a possibility of network-vein type mineralization for those mines. The survey in this area was carried out for the purpose of clarifying these problems and the exploration for deep level.

As the results of geophysical survey (IP method), since the anomaly pattern indicated a steeply dipping form in Karılar deposit, it was thought to be a new hydrothermal deposit. A lenticular anomaly zone which might have reflected an ore body in a relatively shallow part was observed in the Karaerik deposit. According to the results of MJTE-11 drilled in this neighborhood, it was assumed that a stockwork of sulfides developed in dacite. The mined part

of the Karaerik ore deposit was considered to be a part of ore shoot.

In the depths of these ore deposits, IP anomalies different from that in shallow parts were observed. As the results of drilling survey, it is thought that the anomalies of deep level reflected mostly montmorillonite in rhyolite in Karaerik and a pyrite stockwork in dacite of Kızılkaya Formation in Karılar. Geologically speaking, considering that a new thick stratum accumulates toward the north and no remarkable IP anomaly has been observed, it is thought that there is little possibility of existence of Lahanos type massive sulfide ore deposit exists at least shallow than 300 to 400m below the surface of the earth.

5-2 Recommendation in the Future Projects

According to the results obtained through the survey in phase I to III, the following was clarified.

- * Two types of mineralization have been recognized in this area. Those are a massive sulfide type and a stockwork-vein type mineralization (late stage).
- * The mineralization and alteration zones in footwall dacite are widely distributed in the NE-SW direction.
- * The distribution and continuity of the ore horizon of massive sulfide were clarified.
- * The existence of a relatively thick layer of hanging wall tuff is desired in order that an ore body exists.
- * The IP method is effective to explore the area covered with a hanging wall.

Based on the above, the following program will be proposed in the future projects.

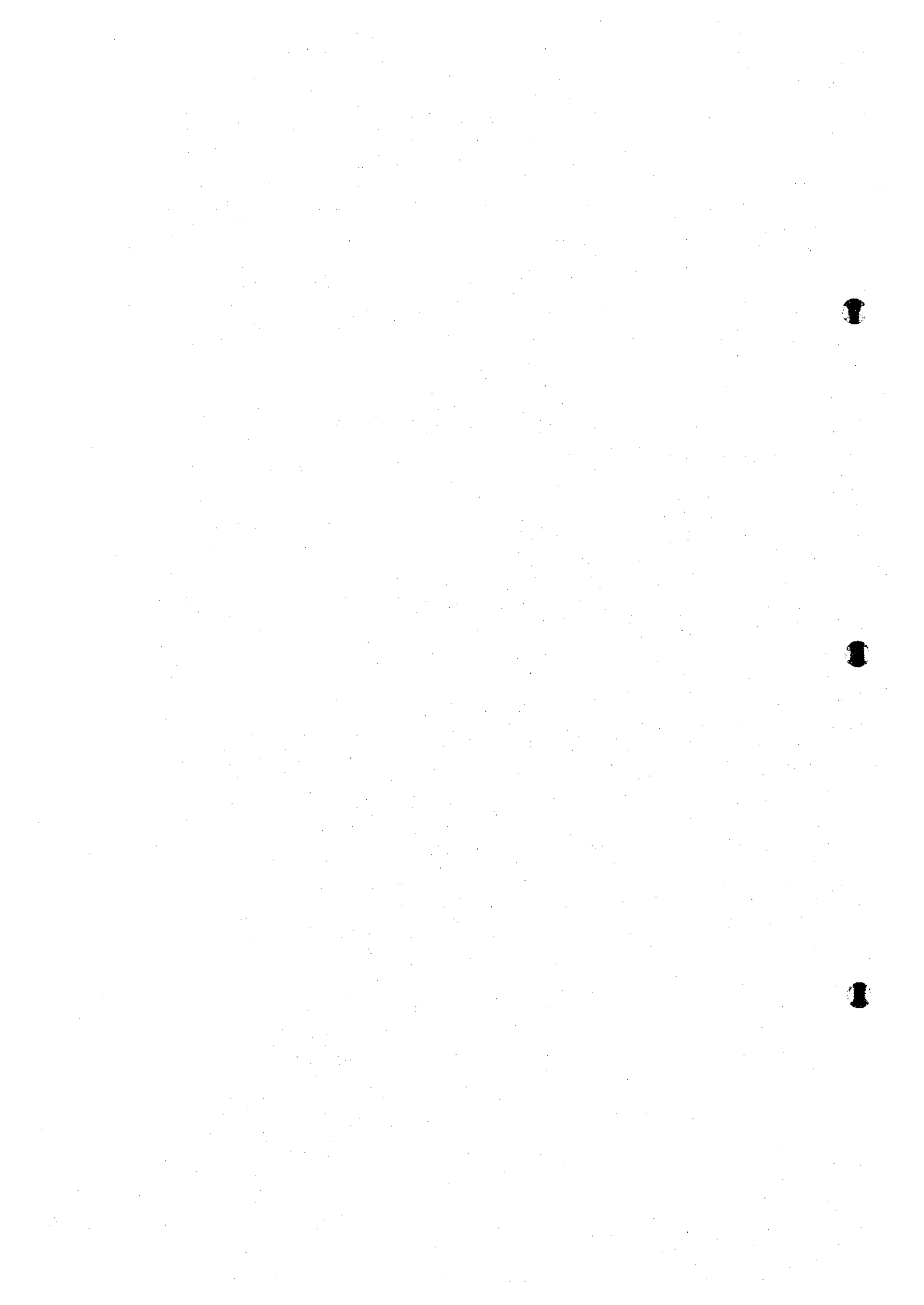
The exploration for promising areas is almost completed, but an economical ore deposit was not discovered. The drilling survey was not conducted only in the Çalkaya area among the promising areas. Since the hanging wall is thick in the Çalkaya area and the exploration depth was not sufficient for the IP survey ($a=100\text{m}$) conducted in phase II survey, it is advisable to carry out an exploration of $a=200\text{m}$ executed in the Karılar area and then make a confirmation by the drilling survey.

There are various types of dacite composing footwall (Kızılkaya Formation). The present survey could not clarify the characteristics of dacite related to the ore deposit. Therefore, it is desirable to make a detailed survey on this dacite, classify lithofacies, and clarify their mineralogical and geochemical characteristics, form, structure, etc. Thus, it is expected that an approach to the massive ore body will be easily.

It is possible that some ore showings of the massive sulfide type ore deposits along the coast of the Eastern Black Sea may contain stockwork type mineralization which became clear through the survey of this area. Therefore, taking into consideration the continuity of the ore

horizon, characteristics of footwall dacite, etc., we suggest a re-investigation of the promising areas in the Eastern Black Sea Region.

PART II Details of the Survey



PART II Details of the Survey

Chapter 1 Geophysical Survey

I-1 IP Survey

I-1-1 Method of the Survey

1. Content of the Survey

The survey areas for electric survey (IP survey) were established in the area concluded to be hopeful by phase I, II survey. Location of the area are shown in Fig.II-1-1~2. Specification of geophysical survey is shown in Table II-1-1.

Table II-1-1 Specification of the IP Survey

Method	Induced polarization method (IP method)
Detection method	Time domain Method
Electrode arrangement	Dipole-Dipole
Separation of electrode arrangement	a=200m,100m
Coefficient of electrodes separation	n=1-4
Number of survey line	7
Total length of survey line	21.4km
Tests of physical property of rocks and ores (laboratory test)	23 specimens for chargeability and resistivity

2. Operation of the Measurements

1) Determination of survey line and survey

Survey lines were planned to start from the well known peak. Open traverse method was adopted to locate exact survey points. Locations of each survey lines are shown too in Fig. II -1-2.

2) The principle of IP method

When the electric current is sent into the earth, various electric chemical phenomena occur in the medium that composes the ground. IP method measures the following two phenomena.

[Over Voltage Effect]

Sending the electric current makes superficially electric two multi-layer on the surface of sulphide and metal conductors. And an electric discharge occurs to opposite direction as switching off an electric current. This phenomenon is occurred by the complex effect of ion and electron conduction. The origination in this phenomenon is the mineral with an electron

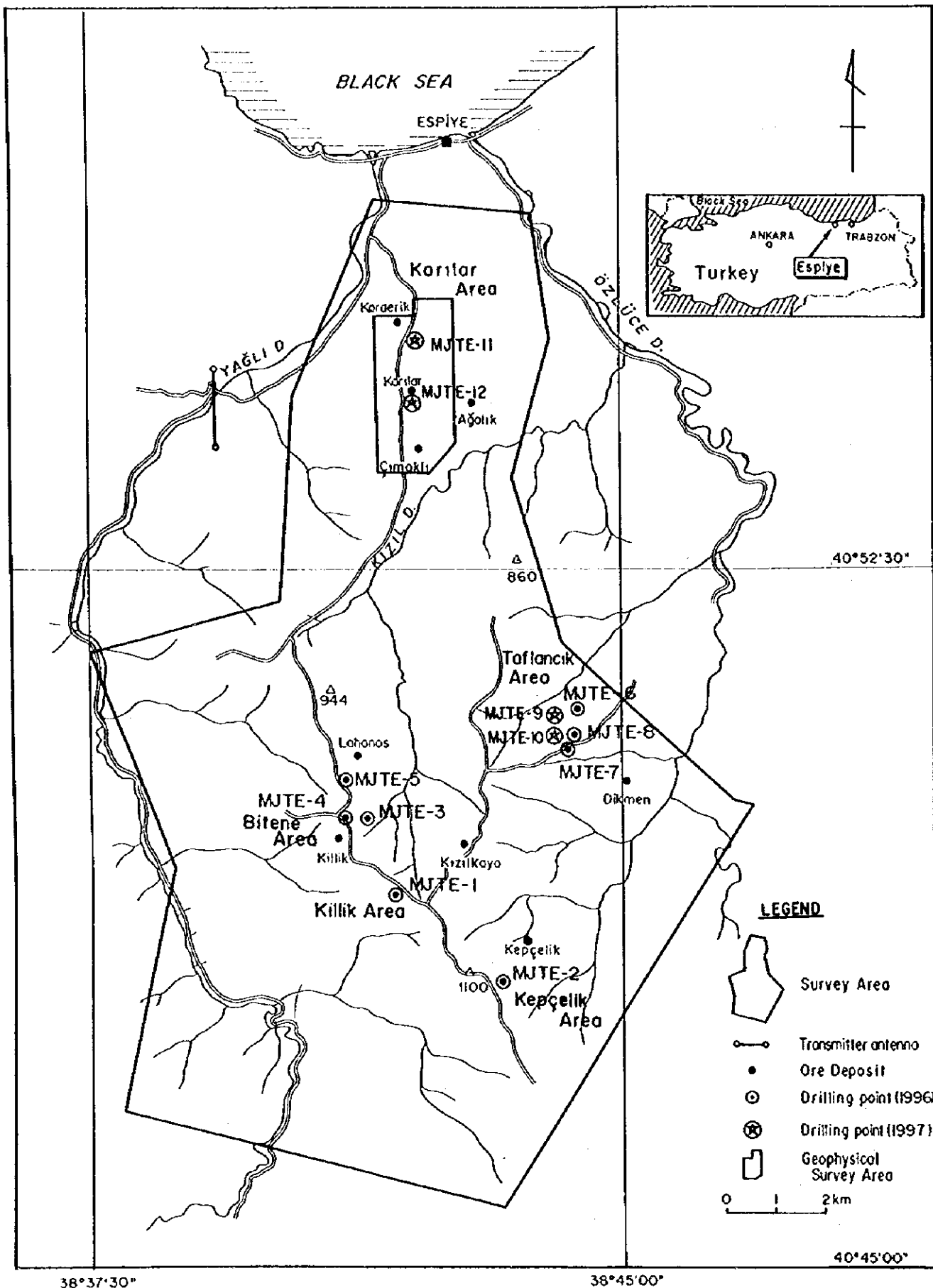


Fig.II-1-1 Location of the Geophysical Survey Area

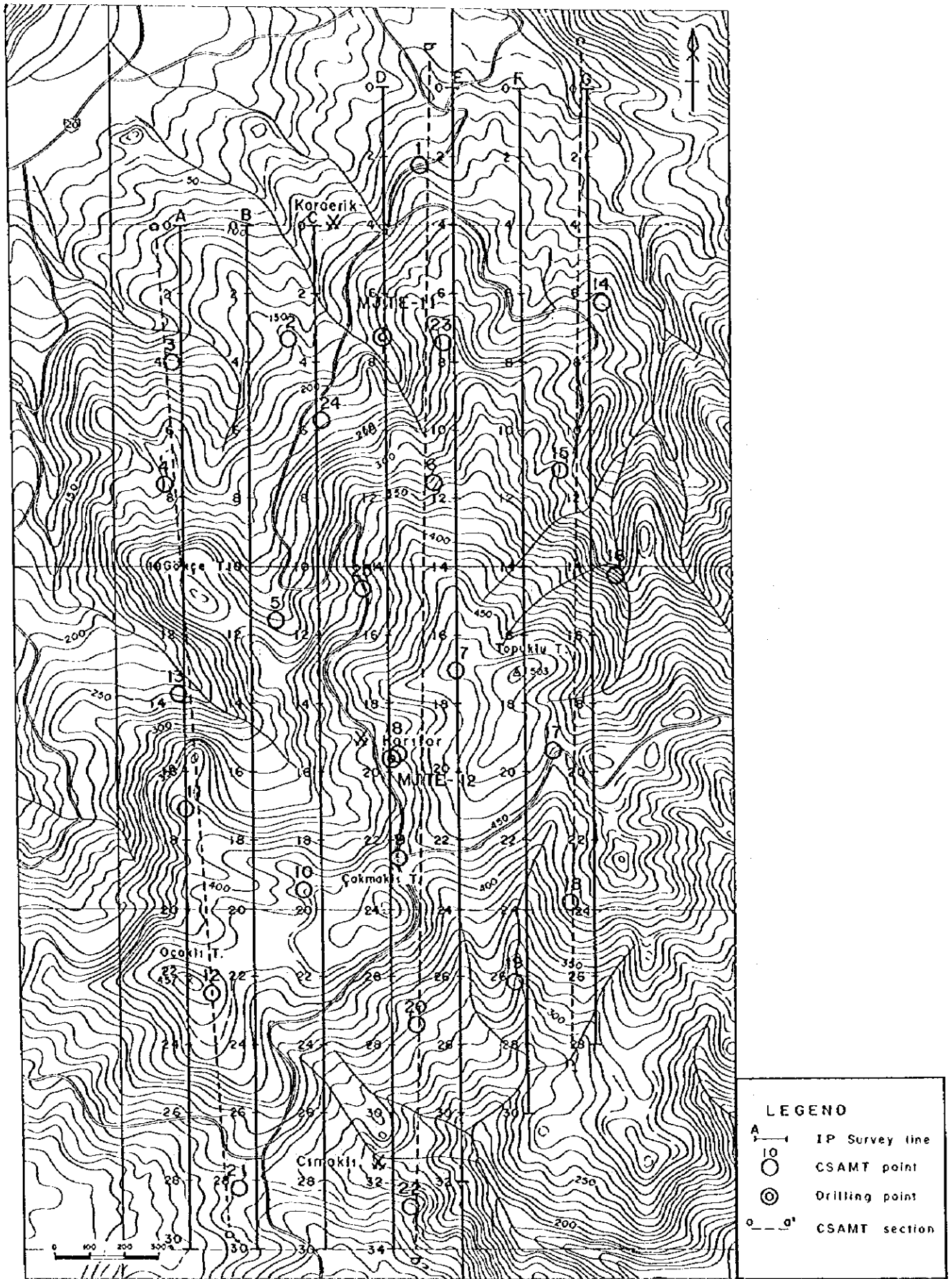


Fig.II-1-2 Location of the IP Survey Lines and CSAMT

conductivity and is too the survey object of IP method.

[Normal Effect or Background]

Polarization occurs by sending an electric current in ordinary rocks. The main origination of this phenomenon is membrane polarization caused by a small quantity of mixed clay minerals. The membrane polarization of montmorillonite is the most largest of all of the various clay minerals and kaolinite is small. The membrane polarization is maximum when there is 5% capacity ratio of clay minerals. However, a membrane polarization decreases when the capacity ratio is larger or smaller than 5%.

The maximum value of membrane polarization is about 5% capacity ratio in the montmorillonite stone quantity, if expressing it with FE value it is about 2%.

This value is extremely small compared to above-mentioned Over Voltage Effect in the sulphide minerals.

3) Measuring method of IP phenomenon

The measurement had been carried out by the time-domain method. This method (abbreviation symbol T.D. method, transient IP method) sends an intermittent direct current (on/off 2.0sec) into the ground through a couple of current electrode C1,C2. After that, we get two data from a couple of potential electrodes P1,P2. One is the primary potential difference (V_p) just before switching off an electric current, the other is the secondary potential difference (V_s) during T time (T time is from 60msec to 1,590msec) after switching off an electric current.

In this survey, we had measured V_s during T time after switching off an electric current.

The concept of operation is shown in Fig.II-1-3. The concept of the method of measurement is shown in Fig.II-1-4 and the list of sampling time is shown Table in II-1-2.

IP effective measurement value is generally called with chargeability, expressed with V_s/V_p [mV/V].

The data of secondary potential difference in this survey has not received an influence of the effect of electromagnetic coupling. At this investigation, the chargeability adopted 820-1,050msec data.

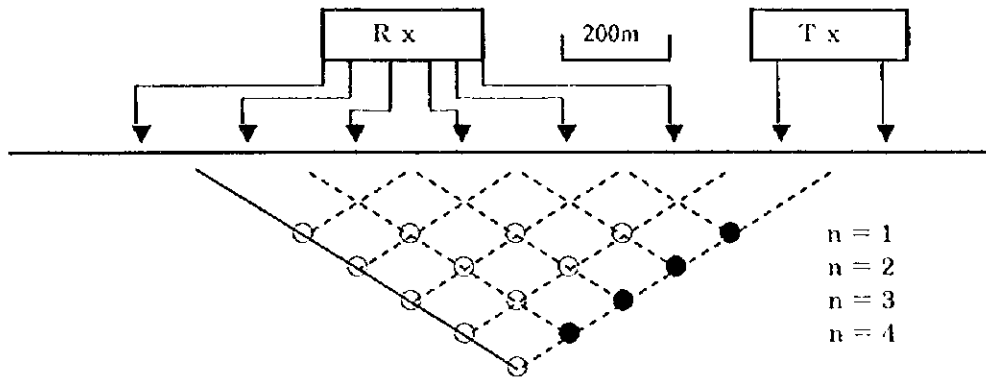


Fig.II-1-3 Concept of IP Operation

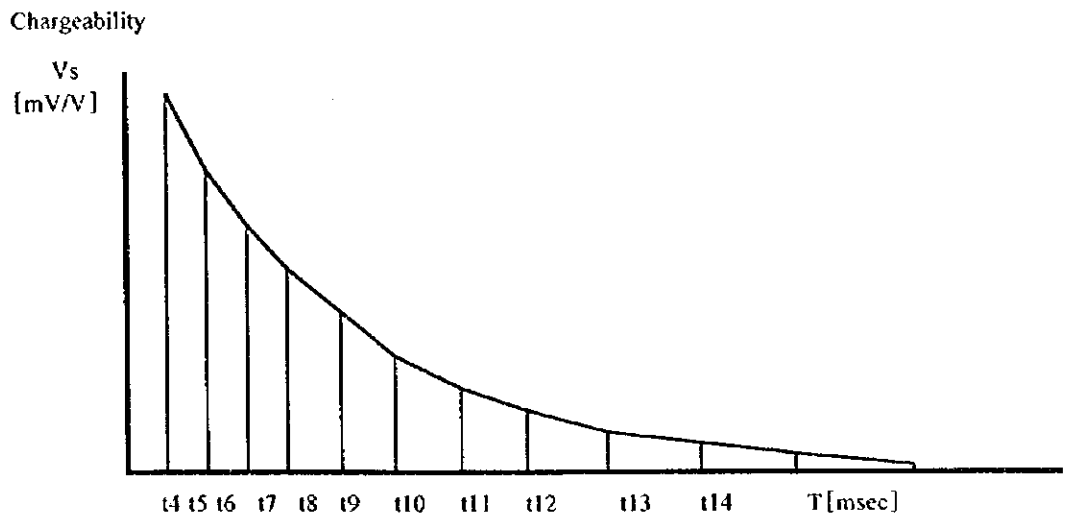


Fig.II-1-4 Concept of the Method of Measurement

Table II-1-2 List of Sampling Time

Slice #	t4	t5	t6	t7	t8	t9	t10	t11	t12	t13	t14
Mid-Point	60	90	130	190	270	380	520	705	935	1230	1590 msec
Width	20	40	40	80	80	140	140	230	230	360	360 msec

3. Measuring Equipment and Materials

The measuring equipment and materials are shown in Table II-1-3.

Table II-1-3 List of IP Equipment and Materials

Field survey

Equipment	Maker	Type	Specification	Amount
*Transmitter	PHOENIX	IPT-2	1500V,15A max output:15KW	1
*Engine Generator	WESTINGHOUSE ELECTRIC	10DE	220V 400Hz 30KW 2 cylinder 4 cycle	1
*Receiver	SCINTREX	IPR-12	8channel, 14window Input Range:50uV to 14V	1
Electrode		Current	stainless steel	1
		Potential	CuSO4	1
Cable	FUJIKURA		VSF1.25mm ² cable	1
Measuring compass	USHIKATA		Pocket compass 100m Esron tape	4
* Communication device	KENWOOD	TH-45G	Output:600mAhW Battery:12V	12

* provided by MTA

Laboratory test

Transmitter	IRIS	IP-L	Output:1uA - 100mA Max 10V	1
Receiver	SCINTREX	IPR-12	8channel, 14window Input Range:50uV - 14V	1
Electrode			Pt	1

4. Method of Analysis

For the analyses of the resistivity and the IP pseudosection, the 2-dimensional inversion program (Zong Corp.) was used. By these analyses the effect of the land form and the typical pattern of dipole-dipole electrode spreading in the depth can be eliminated.

The results of physical property tests of core samples showed that the chargeability had positive correlation to the resistivity. For this reason, a metal factor diagram was prepared. The metal factor (hereinafter referred to as MF) was determined by a formula, that is, $100 \times \text{analyzed resistivity } [\Omega \cdot \text{m}] / \text{analyzed chargeability } [\text{mV/V}]$.

1-1-2 Results of the Survey

1. Results of the Survey

Apparent resistivity and chargeability acquired in this survey are shown in Fig.II-1-5 to 11 as cross sections, Fig.II-1-12 shows apparent resistivity in plan, and Fig.II-1-13 shows chargeability in plan.

1) Cross Section of Apparent Resistivity and Chargeability

There is a distribution of dacite lava of Kızılkaya Formation and dacitic tuff, hematite dacite, rhyolite, porphyritic dacite and nevaditic tuff of Çağlayan Formation. A series of hematite dacite occupies the peak of Mt.Topuklu Tepe, in central part of the area.

The distribution of resistivity can be divided into a high resistivity zone of $100 \Omega \cdot m$ or more and a low resistivity zone of $50 \Omega \cdot m$ or less.

Line A

The high resistivity zone corresponds to the hematite dacite distributing near the site Nos.12, 16-24 on the peaks of the mountains.

The low resistivity zone mainly corresponds to the tuff and rhyolite of Çağlayan Formation. The chargeability shows about 7mV/V at a maximum.

The hematite dacite near site Nos.12 and 24 tends to exhibit a high chargeability corresponding to their high resistivity parts.

Line B

The high resistivity zone corresponds to the hematite dacite distributing near the site Nos. 20-22 on the peaks of the mountains and exhibits a high resistivity of $200 \Omega \cdot m$ or more to the depth.

Low resistivity less than $10 \Omega \cdot m$, was measured both ends of the survey line.

The chargeability is about 5mV/V at a maximum. A high chargeability was observed corresponding to the high resistivity part of the hematite dacite.

Line C

The distribution of high resistivity zone is similar to the measuring line B, but the high resistivity zone of site No.22 is smaller.

The chargeability is about 4mV/V at a maximum. The lowest chargeability was measured on site Nos.4-14 of aphyric dacite lava.

Line D

A high resistivity of about $800 \Omega \cdot m$ was observed with respect to the hematite dacite near site No.12, but a low resistivity of about $30 \Omega \cdot m$ or less was observed in the rest of the area. Especially, near the Karılar (site No.20) and relatively deep part of site No.26 showed low resistivity of $10 \Omega \cdot m$ or less.

A weak and wide anomaly zone of chargeability was observed around site Nos.6-10 (near Karaerik). A weak but clear anomaly of chargeability like pantaloons shape was observed site No. 19 (near Karılar).

Line E

A relatively high resistivity ($50-200 \Omega \cdot m$) was observed near site Nos.18-20 where hematite dacite distribute, but the rest of the part showed a low resistivity of about $30 \Omega \cdot m$ or less.

The chargeability in this line is $7mV/V$ at a maximum. A weak anomaly of chargeability like a half pantaloons shape was observed near site No.6 (near Kraerik deposit).

A weak but relatively clear anomaly like a pantaloons shape was observed in the shallow part of site No.18 (eastward extension of Karılar), where high resistivity hematite dacite distribute.

Line F

The resistivity was found to be low in the region with distribution of Çağlayan formation, and was found to vary within $20-300 \Omega \cdot m$ in the depth of site Nos.10-22 with hematite dacite distribution.

Maximum chargeability of $8mV/V$ was measured. It showed a slightly increasing tendency towards the depth.

Line G

Maximum resistivity of $200 \Omega \cdot m$ was measured in the hematite dacite zone near site No.16.

Maximum chargeability of about $7mV/V$ was measured. High chargeability tend to be observed corresponding to the high resistivity part of the hematite dacite.

2) Plans of Apparent Resistivity and Chargeability

In the case where $n=1$ representing relatively shallow level, most part showed high resistivity reflecting the hematite dacite distribution. In the same lithofacies distribution region, low resistivity was observed only in the valley lying in the west side of Karılar deposit and the valley lying in the northeastern end of the surveyed area, so that it can be considered that the results of the survey represent the lithofacies at a relatively deep level measured with an electrode spacing of 200m.

The results of the survey are shown in Table II-1-4

LINE-B

OBSERVED



Fig.11-1-6 IP Section of Apparent Resistivity and Chargeability (Line B)

LINE-C OBSERVED



Fig. II-1-7 IP Section of Apparent Resistivity and Chargeability (Line C)

LINE-E **OBSERVED**

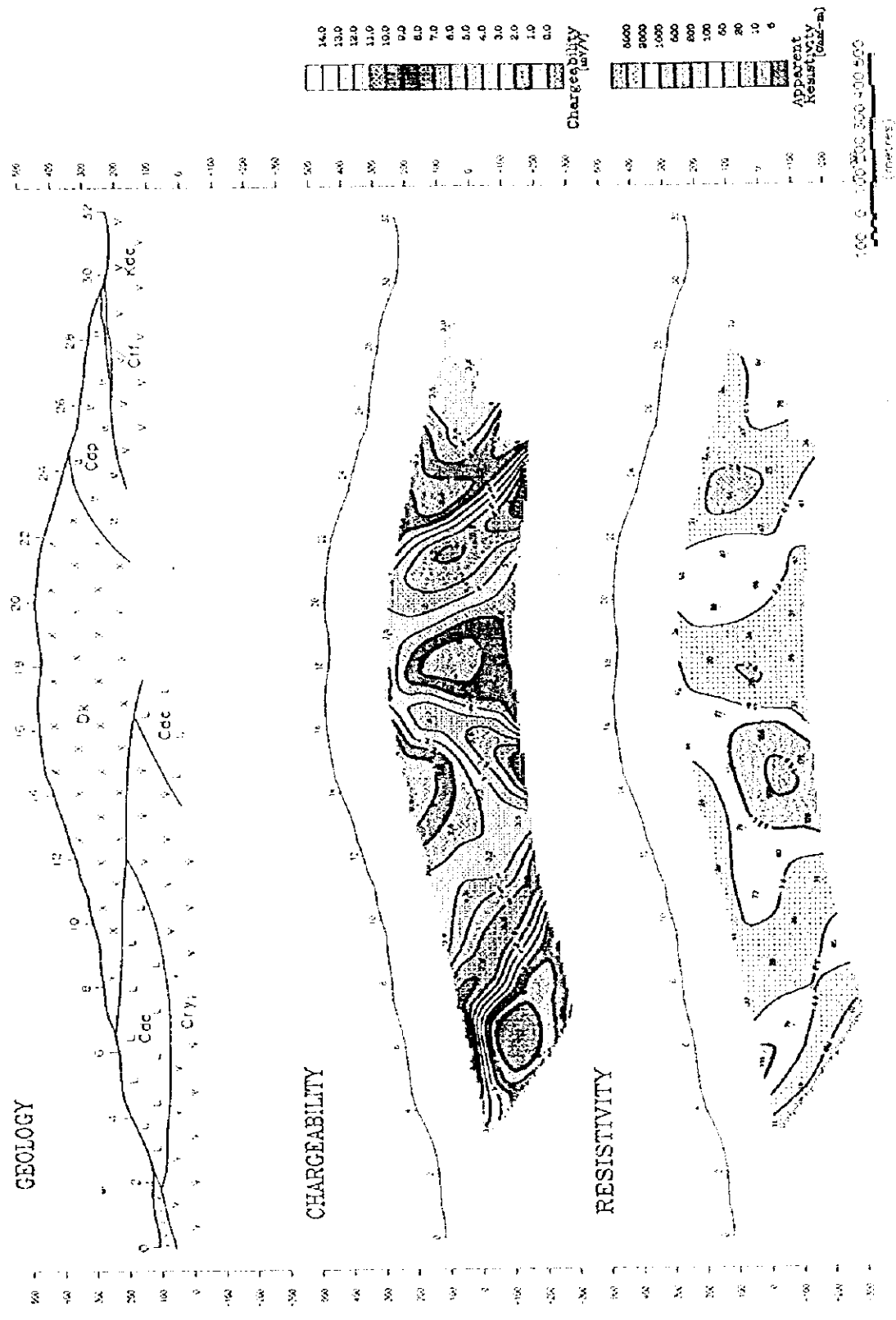


Fig.H-1-9 IP Section of Apparent Resistivity and Chargeability (Line E)

LINE-F

OBSERVED

Topoklu T.

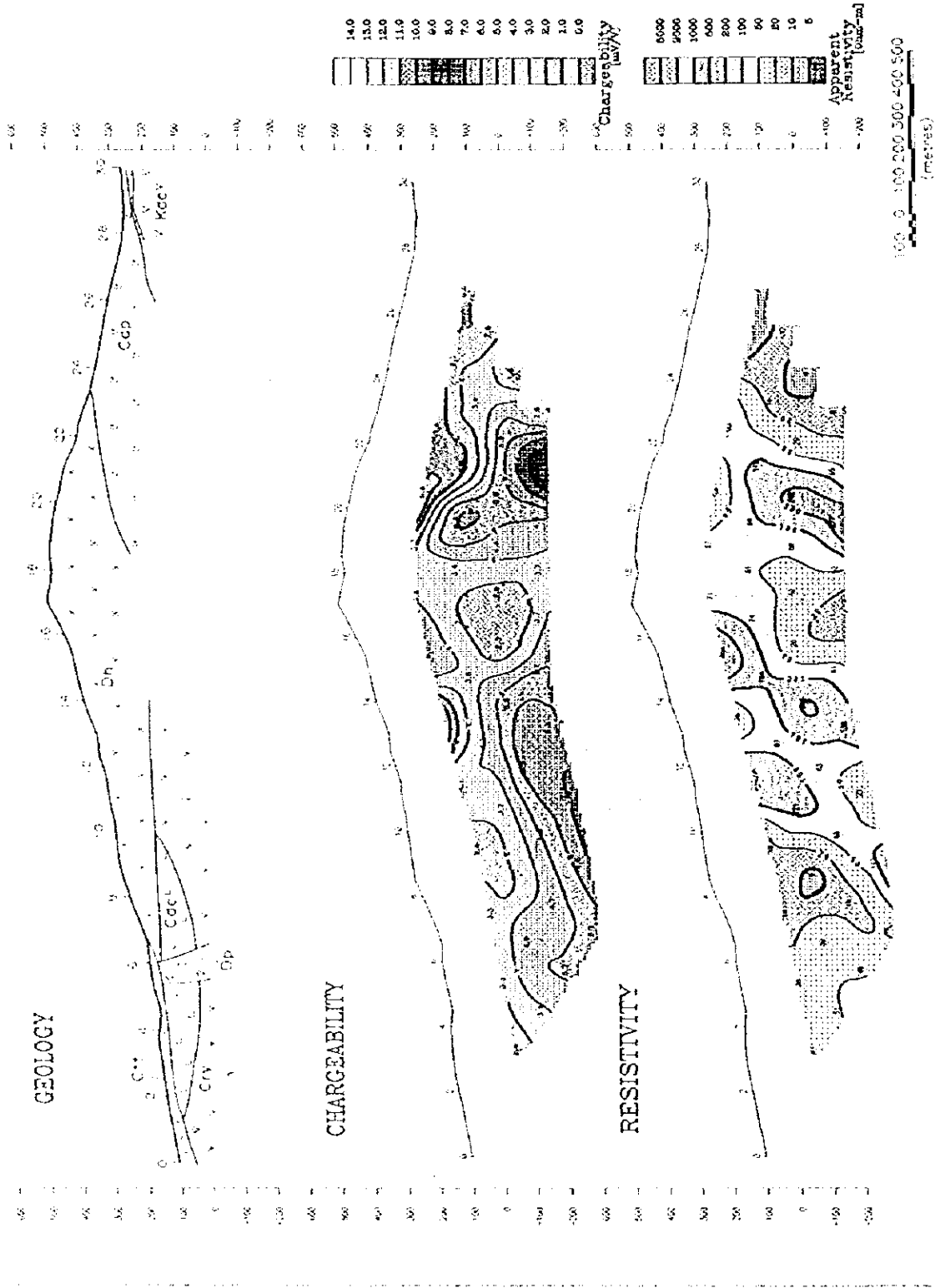
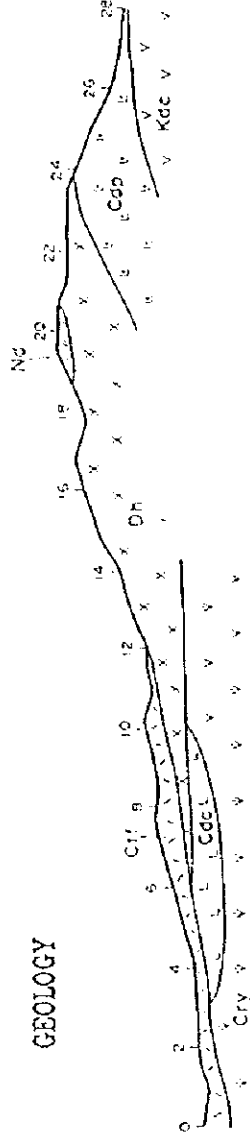


Fig.II-1-10 IP Section of Apparent Resistivity and Chargeability (Line F)

LINE-G

OBSERVED

GEOLOGY



CHARGEABILITY



RESISTIVITY

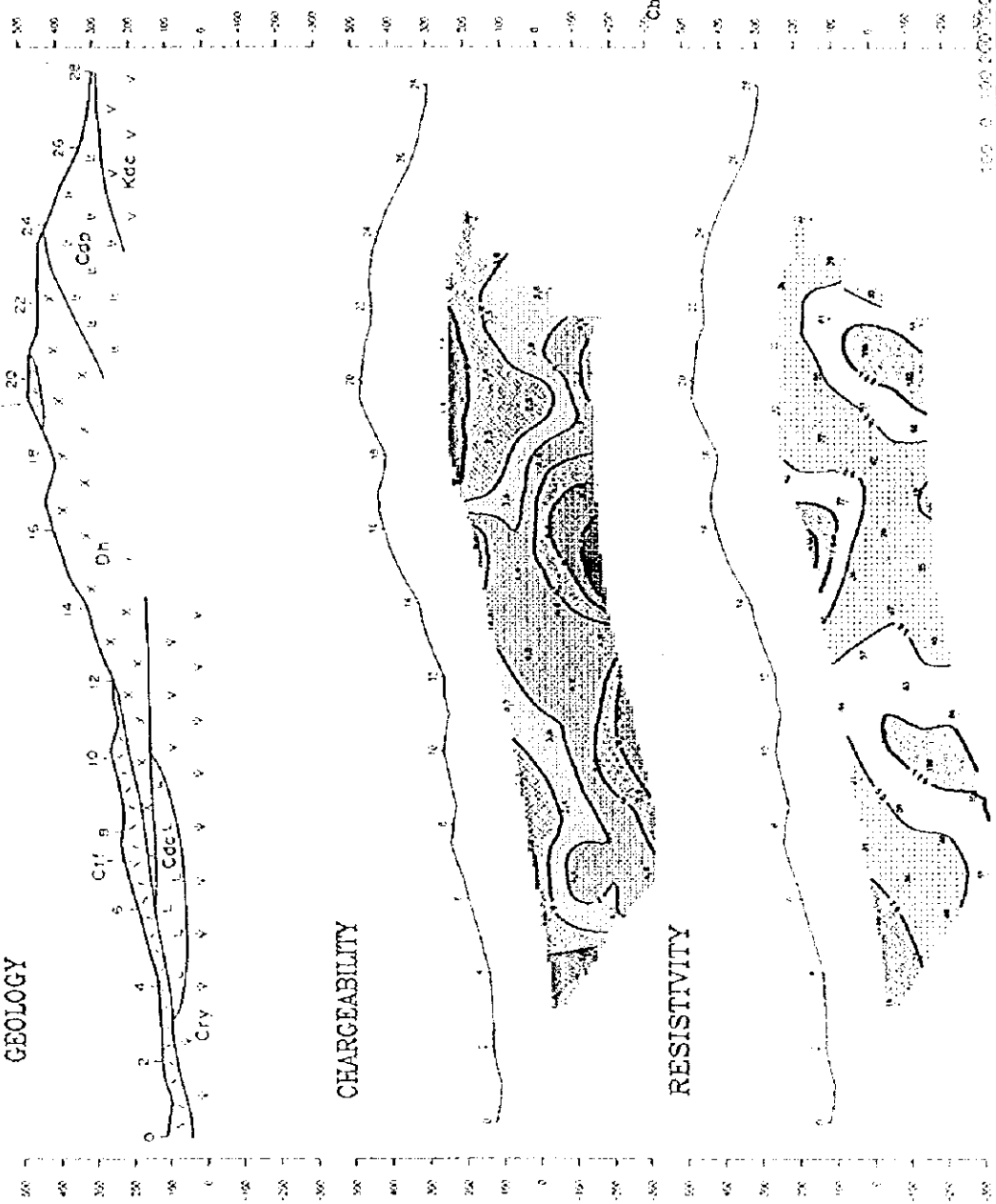
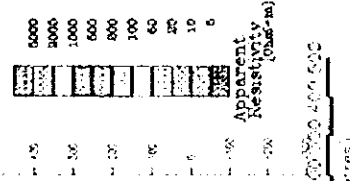


Fig.II-1-11 IP Section of Apparent Resistivity and Chargeability (Line G)

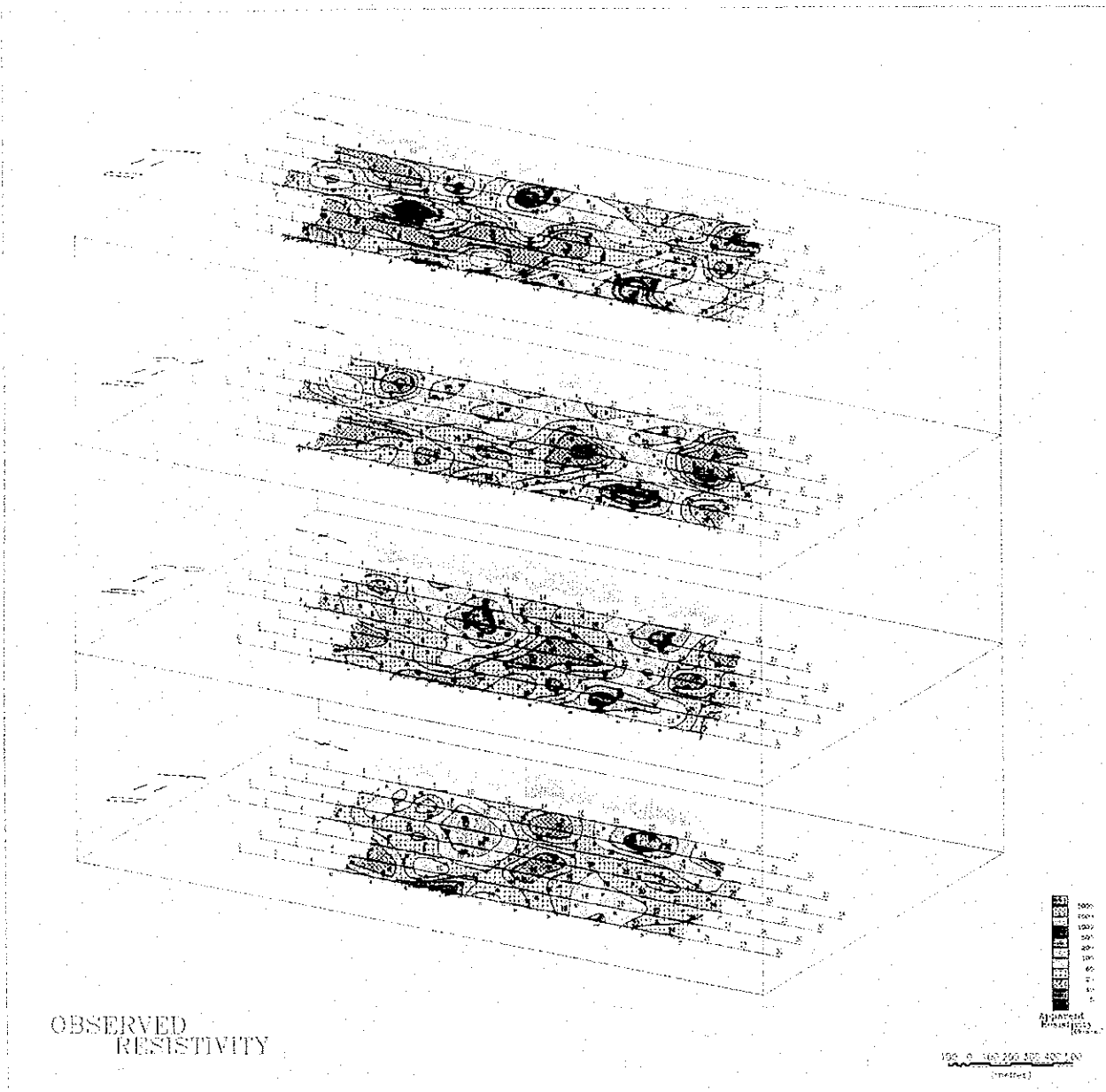


Fig.II-1-12 IP Plane Map of Apparent Resistivity

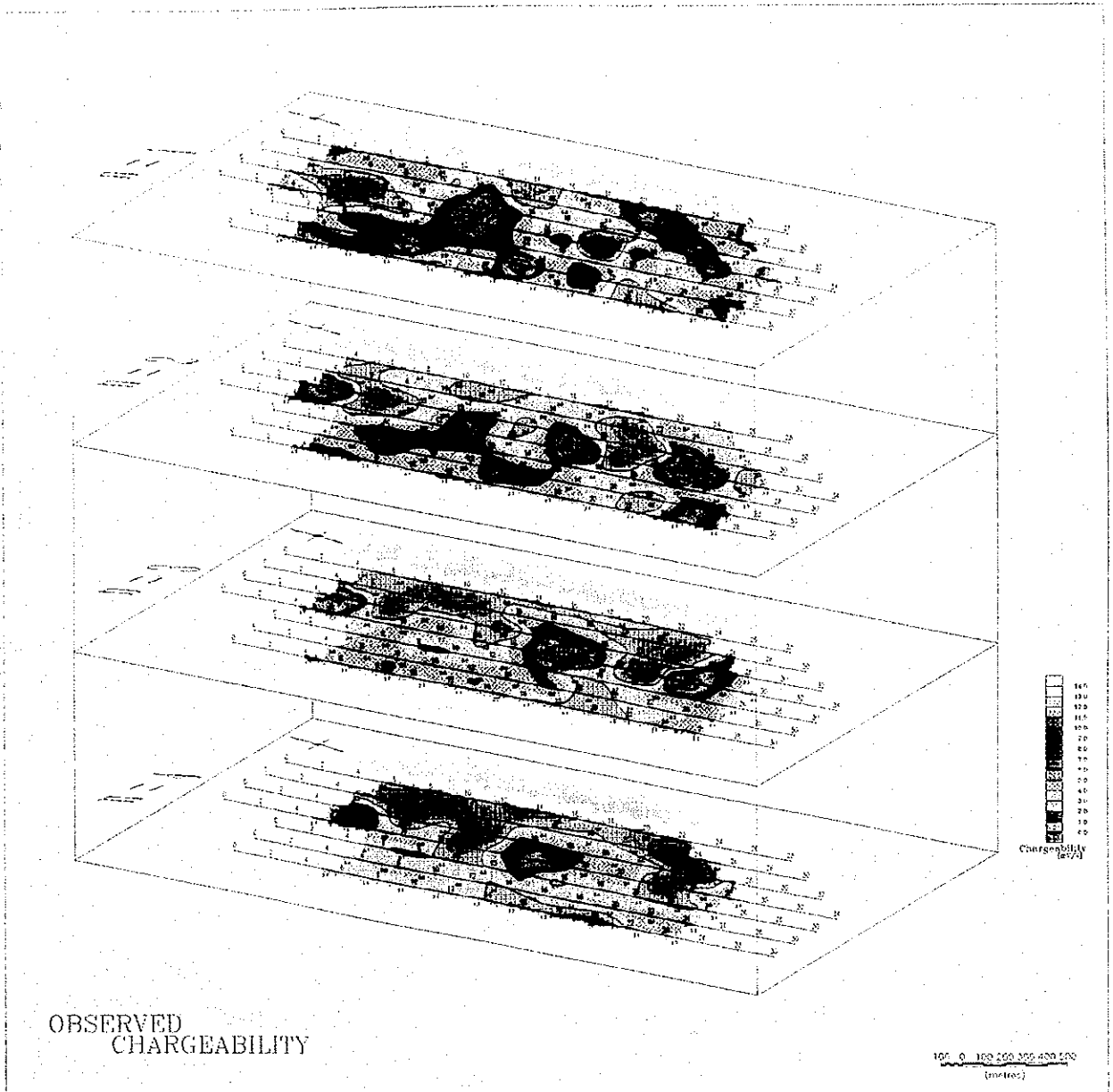


Fig.II-1-13 IP Plane Map of Apparent Chargeability

Table II-1-4 Results of IP Survey

Survey Line	Apparent Resistivity ($\Omega \cdot m$)	Chargeability (mV/V)	Characteristics of IP Distribution Pattern
A	4 ~ 405	0.6 ~ 7.6	A tendency of high chargeability in high resistivity part. No anomaly.
B	10 ~ 440	-0.8 ~ 4.9	A tendency of high chargeability in high resistivity part. No anomaly.
C	9 ~ 181	1.1 ~ 4.3	Tendency of resistivity distribution is almost similar to line B . No anomaly.
D	5 ~ 608	-2.9 ~ 9.8	In site Nos.20-22, definite but weak chargeability anomaly.
E	15 ~ 207	-0.1 ~ 7.5	Weak but clear anomaly in site Nos.6-8 near Karaerik and Kırılar.
F	6 ~ 352	0.5 ~ 8.9	A tendency of high chargeability in high resistivity part. No anomaly.
G	14 ~ 213	0.8 ~ 7.8	A tendency of high chargeability corresponding to high resistivity No anomaly.

2. Results of Physical Property Test

1) Method for the Test

In order to obtain the basic data of the electric characteristics of the drilling core, the resistivity and chargeability were measured with respect to 23 pieces of representative samples. Sample were soaked in water ($100 \Omega \cdot m$) for a day after cubing cut. Sampling was made from relatively hard portions in order to prevent the samples from being broken in the water during the test.

2) Employed Equipment

List of employed equipment for the test is shown in Table II-1-3.

3) Results of the Test

The results of the laboratory test of the drilling core samples are shown in Table II-1-5.

The relationship between the apparent resistivity and chargeability for each of all the samples (1st year through 3rd year) and the relationship between each sample and MF are shown in Fig. II-1-14 and Fig.II-1-15 respectively.

As for the chargeability, the rhyolite at the depth of 247m (MJTE-11) showed 32mV/V at a maximum, but no mineralization was observed.

Resistivity value of all samples varies from 9 to 1,300 $\Omega \cdot m$ and strongly depending on the effects of lithofacies and clay mineral. The samples of Çağlayan Formation in general showed a low resistivity of about 50 $\Omega \cdot m$ or less.

Of all the samples, with respect to the rocks other than the ores, the dissemination sample of pyrite in dacite lava (Kızılkaya formation) showed chargeability of 20-100mV/V. Unmineralized samples showed chargeability of about 30mV/V or less. The samples having high resistivity tend to exhibit high chargeability.

On the basis of MF, the rocks and ores are definitely separated by about 100, but those ranging from 100-1,000, belong to the category of weak siliceous ore to low grade black ore.

1-1-3 Results of Analysis

The results of simulating analysis (inversion) are shown in Fig.II-1-16 through 21.

The resistivity distribution according to the result of analysis can be roughly divided into high resistivity zone (about 100 $\Omega \cdot m$ or more) and low resistivity zone (about 50 $\Omega \cdot m$ or less).

The hematite dacite distribution area varies largely, for example, 20-1,700 $\Omega \cdot m$. In such a distribution zone, those parts exhibiting resistivity of about 300 $\Omega \cdot m$ or more can be presumed to having hard and massive property while those parts exhibiting resistivity of about 50 $\Omega \cdot m$ or less can be considered to reflecting the argillic alteration as observed on out crop.

Low resistivity of about 10 $\Omega \cdot m$ or less reflected the strong argillized zone and the tuff with abundant clay minerals.

Section of Simulated Result (Resistivity, Fig.II-1-16)

Line A

The calculated resistivity of hematite dacite near site Nos.8-26 was more than 100 $\Omega \cdot m$ and the thickness of the dacite was estimated to be about 300m at its maximum.

Site Nos.0-7, 14 exhibited 10 $\Omega \cdot m$ or less and well correspond to the distribution of dacitic tuff of Çağlayan Formation containing a large amount of clay minerals.

Line B

In general, the hematite dacite has low resistivity near the surface due to alteration but, high resistivity zone under the Nos.18-24 indicate a large massive body of dacite. The resistivity

in the zone ranging from shallow to relatively deep in site Nos.8-18 were calculated to be about $20 \Omega \cdot m$ or less, which differs hardly from the resistivity of each of the aphyric dacite, dacitic tuff and rhyolite of Çağlayan Formation.

Line C

The low resistivity of $8-30 \Omega \cdot m$ is predominant along this line, and it was reflecting the intense argillic alteration. High resistivity zones corresponding to the hematite dacite in site Nos.22-24 distribute in relatively shallow parts. High resistivity zones at the depth of about 200m or more in site Nos.8-12 are larger in scale than line B, but those lithofacies have not been defined.

Line D

Near the surface of site Nos.10-14 and 26-28 respectively exhibit high resistivity and correspond to hematite dacite distribution zone, the thickness of those high resistivity parts being estimated to be about 300m at its maximum. Low resistivity parts of less than $10 \Omega \cdot m$ scatter in site Nos.8, 14, 17 and 28. Those in site Nos.8, 14 and 17 are considered to belong a low resistivity ($30 \Omega \cdot m$ or less) zone, but the low resistivity exhibited in the depth of site No.8 (near Karaerik deposit) is not clarified whether it results from the effect of mineralization or mere argillization.

The low resistivity zone of (near Karılar deposit) site Nos.14 and 17 is presumed to reflect the weak mineralization of the hematite dacite. Near the boundary between low and high resistibility zones of site No.28 is presumed to reflect the weak mineralization or alteration in upper part of the dacite lava of Kızılkaya Formation.

Line E

High resistivity zone of site Nos.18-20 lie in succession from the surface to the depth on the north side, and this high resistivity zone is considered to be the same zone of high resistivity zone lying at the depth near site Nos.10-16 in lines D and F.

The low resistivity zone ($20 \Omega \cdot m$) around Karaerik deposit was calculated independently on a relatively high resistivity zone ($100 \Omega \cdot m$ or more).

Eastward extension of Karılar ore deposit of site Nos.20-22 lies near the boundary between a low resistivity zone of about $20 \Omega \cdot m$ and a high resistivity zone of $100 \Omega \cdot m$ or more.

Line F

The high resistivity zone corresponding to the hematite dacite is considered to almost coincide with the line E. The high resistivity zone of $1,000 \Omega \cdot m$ or more was calculated at the depth of site No.24, but the comparable geology was not clear. The distribution of low resistivity less than $20 \Omega \cdot m$ near the surfaces of site Nos.4-6 and 10-12 are similar to that of Karaerik

deposit in the line E.

Line G

The high resistivity zone almost coincides with the line F, and no anomaly was observed.

Section of Simulated Result (Chargeability, Fig.II-1-17)

The maximum chargeability value of 17 mV/V was calculated.

Line A

The maximum chargeability (7mV/V) in this line was calculated near the surface of site Nos.12-14 and 24-26. The high resistivity part of hematite dacite tends to show high chargeability.

Line B

Chargeability at a shallow level was analyzed to be 2mV/V or less. The highest chargeability of 12mV/V was calculated at the depth of site No.20. Judging from the resistivity distribution, this chargeability is considered to reflect the presence of a hematite dacite.

Line C

The highest chargeability of about 12mV/V was analyzed at the depth of site No.10. This chargeability is considered to reflect the high resistivity hematite dacite.

Line D

The highest chargeability (about 17mV/V) was analyzed near Karılar deposit of site No. 19. In general, high resistivity zone tends to exhibit a high chargeability. However, the low resistivity and high chargeability zone was found under site Nos.8 and 19. This is considered reflecting the characteristics of mineralization. This portion lies at the depth of about 200m.

Line E

The highest chargeability (about 13mV/V) was obtained near the Karaerik deposit of site No.6 and near the Karılar deposit of site No.19. In general, the higher the resistivity, the higher the chargeability; however, the low resistivity and high chargeability zone was found near the Karaerik deposit of site Nos.4-6. This is considered reflecting the characteristics of mineralization.

Line F

In general, high resistivity zone tends to exhibit a high chargeability, reflecting geology well.

Line G

In general, high resistivity zone tends to exhibit a high chargeability, reflecting geology well.

Plane Map of Simulated Result (Resistivity, Fig.II-1-18)

In the hematite dacite distribution area, the analyzed resistivity near the surface ranging from 10-1,000 $\Omega \cdot m$. The variation of resistivity is considered mainly due to the lithofacies and argillic alteration. A hard and massive hematite dacite has the resistivity of 200 $\Omega \cdot m$ or more. Judging from the distribution of resistivity, the depths of site No.20 of the line B and site Nos. 8-18 of the line F are considered to exist hard and massive rock body.

The resistivity of the rocks except the hematite dacite are considered to be of low resistivity, reflecting their argillization.

Concerning the resistivity of the Karaerik deposit and that of the Karılar deposit, both of these deposits are near the boundary between high resistivity zone and low resistivity zone but do not fall within extremely low resistivity zone.

Judging from the low resistivity distribution in deeper than 100m, It is considered that the low resistivity zone extending approximately east to west below the Karaerik deposit and Karılar deposit respectively.

Plane Map of Simulated Result (Chargeability, Fig.II-1-19)

Concerning the chargeability near the surface of Karaerik deposit and Karılar deposit, the both definitely correspond to a weak anomaly of chargeability zone.

It is considered that, in the case of Karaerik deposit, the anomaly zone of chargeability is limited to shallow level, whereas, in the case of the Karılar, the anomaly zone extends to a relatively deep level.

The high chargeability zones except around ore deposits tend to exhibit a high resistivity and this can be considered reflecting the effect of intrusive rock.

Section of Simulated Result (Metal Factor, Fig.II-1-20)

The data on the ends of survey lines are not actually measured data, so that they are not included in the result of analysis but will be discussed in the following. The obtained data of MF values are considered to be relatively low. Since the electrode spacing for exploration to the deep level, in general, the apparent MF values become low, so that typical cases of the MF distribution are listed below.

Line D

Site Nos. 8-10: Inclination plate shape, MF is 65 at the depth of about 100-250m.

Site No. 20: Inclination plate shape, MF is 76 from surface to deep level.

Site Nos. 24-26: Inclination plate shape, MF is 26 at the depth of about 300m.

Line E

Site Nos.4-6: Lens shape, MF is 100 at the depth of about 100m.

Line F

Site No.27: Lens shape MF is 196 at the depth of about 80m.

Plane Map of Simulated Result of Metal Factor (Fig. II-1-21)

Considering the relationship between MF distribution and the ore deposits of Karaerik and Karılar, the values of MF tend to rise slightly in a wide area at shallow level near the ore deposits. No anomaly of MF was observed at deep level.

In the case of Karaerik deposit, the weak MF zone is not detectable at deep levels, whereas, in the case of the Karılar deposit, the weak MF zone becomes obvious at the depth of 50m or more and continues to a relatively deep level.

To the levels of 50-200m deep, a weak but relatively high MF can be observed near the site No.27 at the south end of the line F. This weak anomaly is considered reflecting the presence of a weak mineralized zone from the top of the dacite lava of Kızılkaya Formation to the aphyric dacite of Çağlayan Formation.

Subdetail IP Survey (a=100m)

In order to clarify the characteristics of the IP anomaly obtained with electrode spacing of 200m, the measurements with the electrode spacing of 100m were carried out in the vicinities of Karaerik and Karılar deposit on part of the measuring line D and E.

The results of measurement and analysis are summarized in Fig.II-1-22 (Line D) and Fig.II-1-23 (Line E).

Through the measurement by the electrode spacing of 100m the characteristics of the IP anomalies have been clarified in detail.

It is found that both the Karaerik and Karılar showed obvious IP anomaly, but the value of the chargeability is as low as about 30mV/V at a maximum. Further, the result of analysis and the characteristics of the MF distribution suggest that the ore deposit form the Karaerik is of a lens shape, while that of Karılar mine is of a vein shape.

Results of the analysis are shown in Table II-1-6 .

Table II-1-5 Results of Physical Property Tests

Drilling No.	Geology	DEPTH(m)	RHO(ohm-m)	M12:820~1,050msec													
				M4	M5	M6	M7	M8	M9	M10	M11	M12	M13	M14	MF		
TE-9	Dh	90.0	164.8	11.92	10.63	8.84	7.75	6.77	5.47	4.93	4.58	4.22	3.57	2.8			
	Kt2	148.9	60.1	27.41	23.21	20.99	18.75	16.51	14.41	12.40	10.57	8.88	7.40	17.6			
	Dp	190.0	159.7	29.03	24.57	20.88	17.44	14.43	11.82	9.60	7.72	6.17	4.91	3.90			
	Kt1	220.0	75.5	35.34	31.91	28.81	25.56	22.40	19.31	16.45	13.79	11.44	9.37	7.60			
TE-10	Dp	85.6	56.5	17.52	15.67	14.22	12.85	11.50	10.17	8.90	7.68	6.55	5.50	4.58			
	Kdc	108.5	34.0	11.51	9.22	7.48	6.00	4.81	3.92	3.31	2.90	2.68	2.55	2.47			
	Kt2	138.0	80.7	24.60	21.67	19.37	16.99	14.54	12.42	10.40	8.63	7.11	5.89	4.76			
	Kdc	195.5	190.6	13.39	11.20	9.50	7.98	6.70	5.64	4.80	4.10	3.55	3.08	2.89			
TE-11	Kdc	219.5	171.1	6.02	4.73	3.82	3.07	2.53	2.16	1.95	1.84	1.79	1.78	1.76			
	Kt1	245.0	104.1	13.70	10.13	7.46	5.24	3.48	2.17	1.27	0.70	0.39	0.29	0.34			
	Cdc	40.0	28.3	61.25	57.42	52.65	46.71	40.27	33.61	27.15	20.99	15.47	10.76	6.93			
	Cdc	105.0	85.2	8.75	5.30	3.25	2.08	1.61	1.64	1.97	2.42	2.88	3.23	3.44			
TE-12	Cdc	171.0	57.6	24.58	24.19	22.67	20.22	17.31	14.11	10.98	7.96	5.31	3.07	1.31			
	Dp	202.9	25.0	47.67	45.06	41.39	36.70	31.60	26.23	21.03	16.08	11.66	7.89	4.87			
	Cry	247.0	23.4	99.92	93.11	85.84	77.27	68.31	58.89	49.64	40.65	32.40	25.00	18.78			
	Cry	329.0	24.3	58.04	54.86	50.95	46.36	41.35	35.95	30.55	25.29	20.37	15.88	11.97			
TE-12	Dp	391.5	24.0	24.46	21.10	18.74	16.71	14.94	13.34	11.91	10.64	9.50	8.44	7.48			
	Dh	34.7	29.8	82.83	68.50	57.53	48.45	41.17	35.07	29.99	25.59	21.80	18.50	15.68			
	Dh	61.0	151.7	5.51	5.62	5.36	4.89	4.32	3.66	2.98	2.28	1.82	1.01	0.49			
	Dh	175.0	18.0	32.91	26.52	21.52	17.27	14.04	11.83	10.32	9.29	8.84	8.01	7.58			
ORE (Kariar)	Ctf	237.5	24.9	43.82	34.58	27.86	22.55	18.46	15.26	12.82	10.85	9.20	7.80	6.81			
	Cdc	288.0	9.0	11.37	10.89	10.78	10.53	10.12	9.85	9.35	8.90	8.39	7.82	7.29			
	Kdc	350.0	302.7	5.48	5.14	4.34	4.24	3.93	3.44	2.89	2.29	1.72	1.21	0.78			
	Py	159.5	418.32	384.19	349.05	310.39	271.99	234.33	199.34	166.81	137.83	112.20	90.34	88.4			
		114.7	409.55	376.89	343.17	305.87	268.66	231.98	197.81	165.97	137.62	112.56	91.18	120.0			
		99.0	405.60	372.46	338.81	302.21	266.14	230.91	198.19	167.66	140.30	115.87	94.86	141.7			
		37.4	772.26	747.56	719.09	683.65	644.46	601.34	558.99	510.77	484.80	418.69	374.11	1241.7			
		20.2	885.98	885.47	840.86	808.53	770.90	726.77	679.88	629.85	578.56	525.88	474.67	2862.9			
		57.9	733.78	706.40	675.43	637.98	597.69	554.87	512.23	469.52	428.74	389.53	353.00	740.2			

Cdc: Porphyritic dacite lava
 Ctf: Dacitic Pyroclastics
 Cry: Rhyolite

Kdc: Dacite Lava
 Kt2: Dacitic Pyroclastics
 Kt1: Dacite tuff breccia

Dp: Porphyritic Dacite
 Dh: Hematitic Dacite

MF : M12/Rho*100

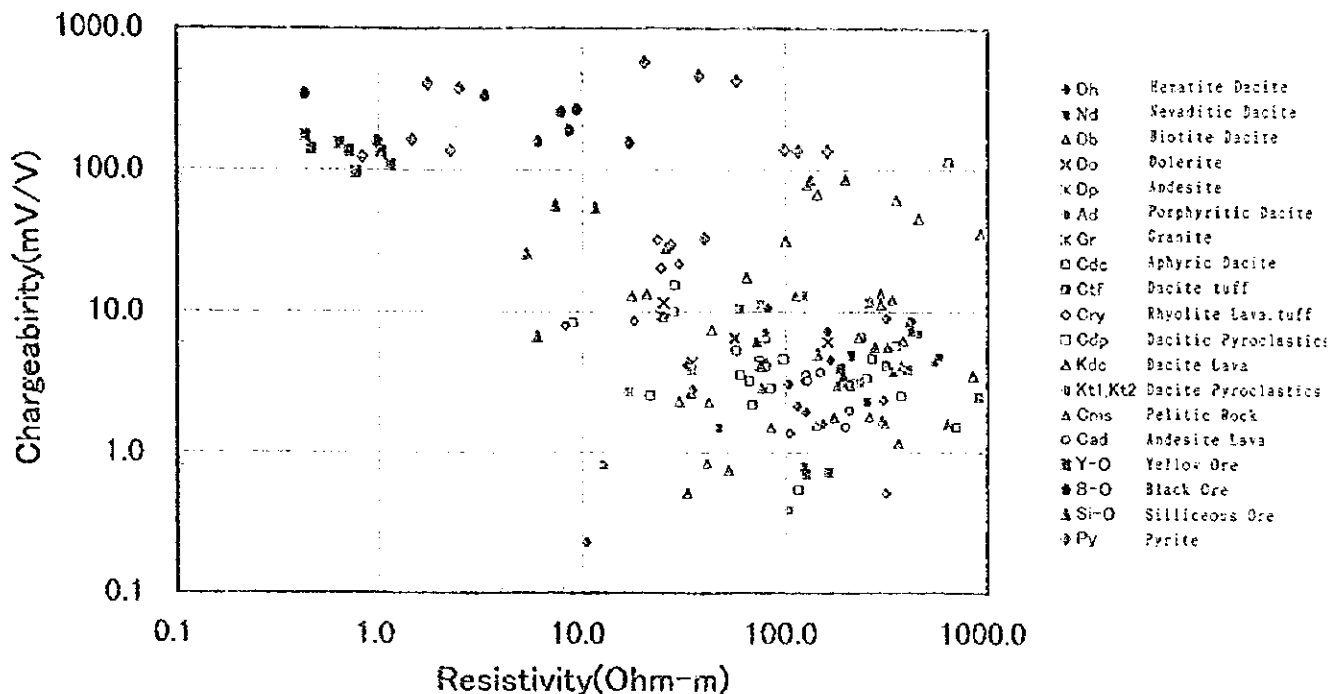


Fig.II-I-14 Relation between Apparent Resistivity and Chargeability of Rock and Ore Samples

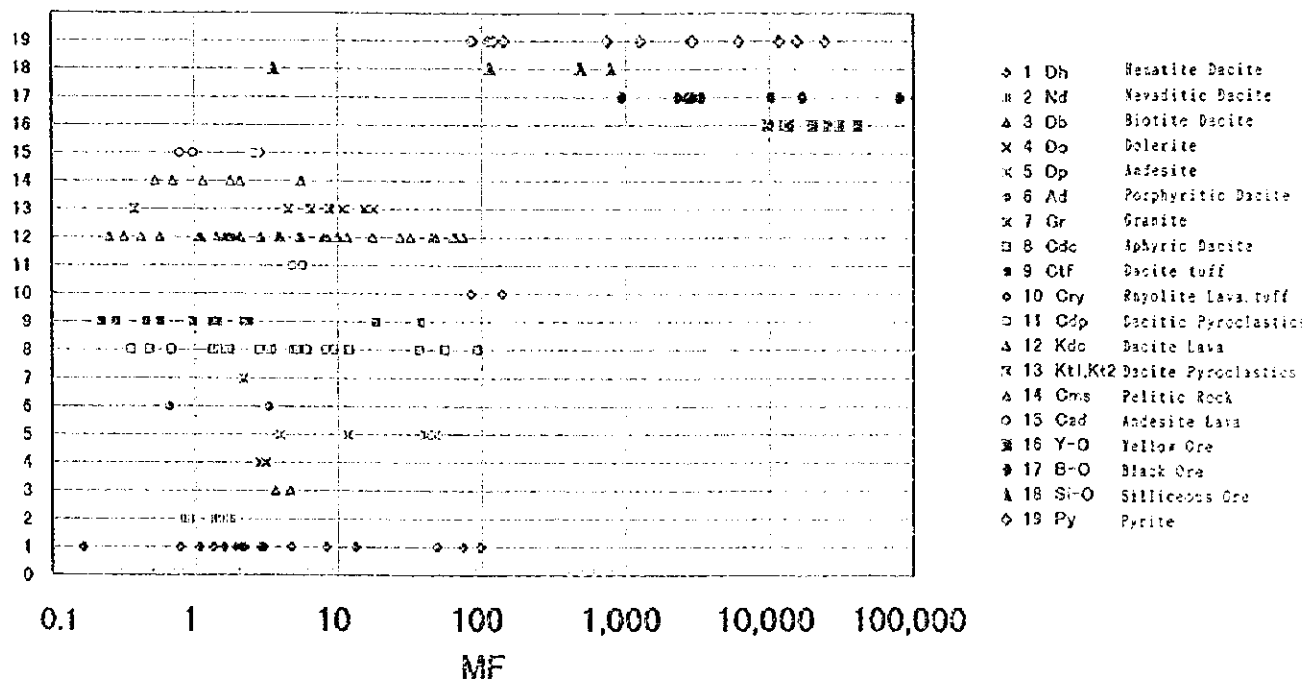


Fig.II-I-15 MF Property of Rock and Ore Samples



APPARENT RESISTIVITY [SMOOTH MODEL]

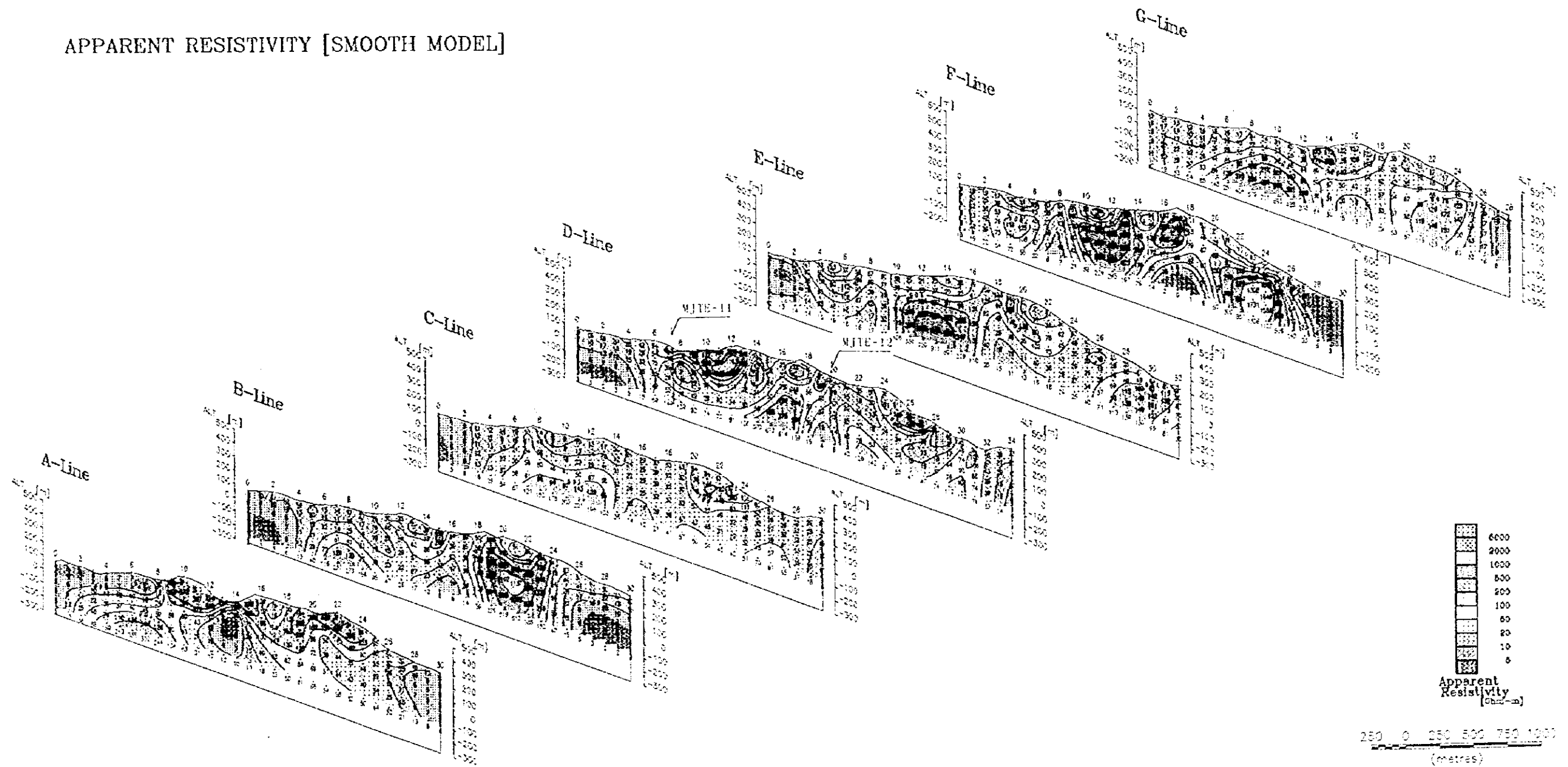


Fig II-1-16 IP Section of Simulated Result (Resistivity)

CHARGEABILITY [SMOOTH MODEL]

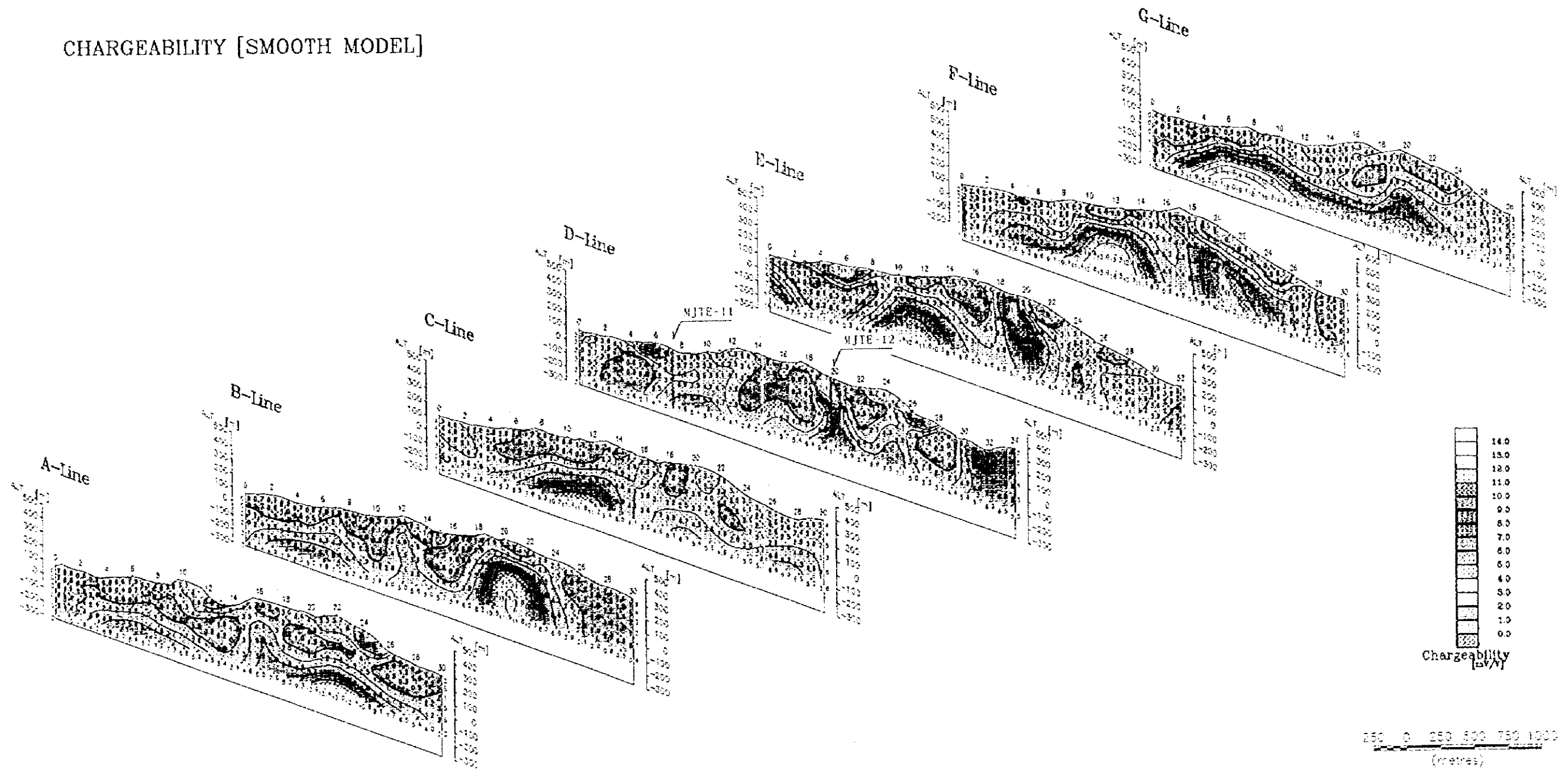


Fig.II-1-17 IP Section of Simulated Result (Chargeability)

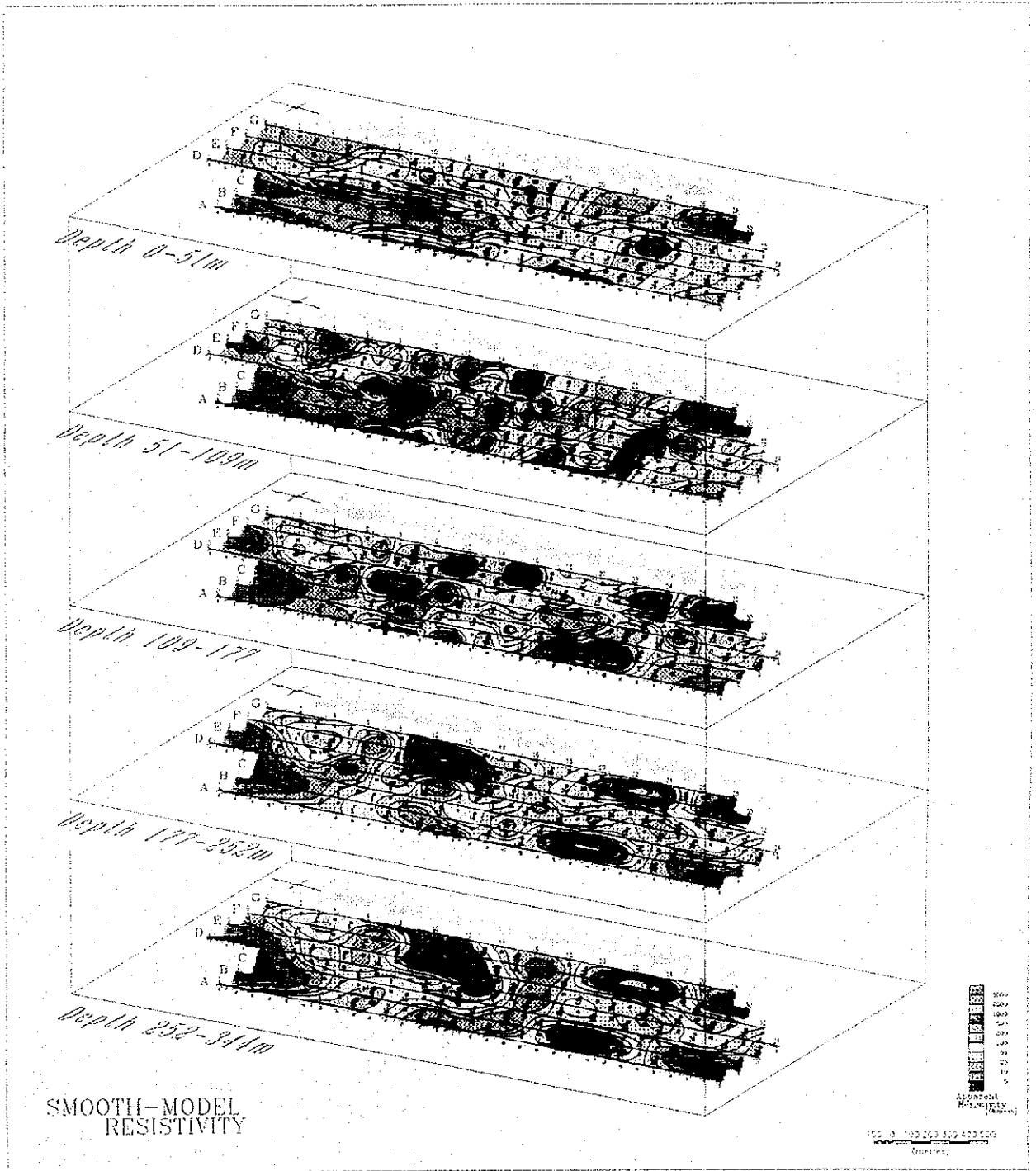


Fig.II-1-18 IP Plane Map of Simulated Result (Resistivity)

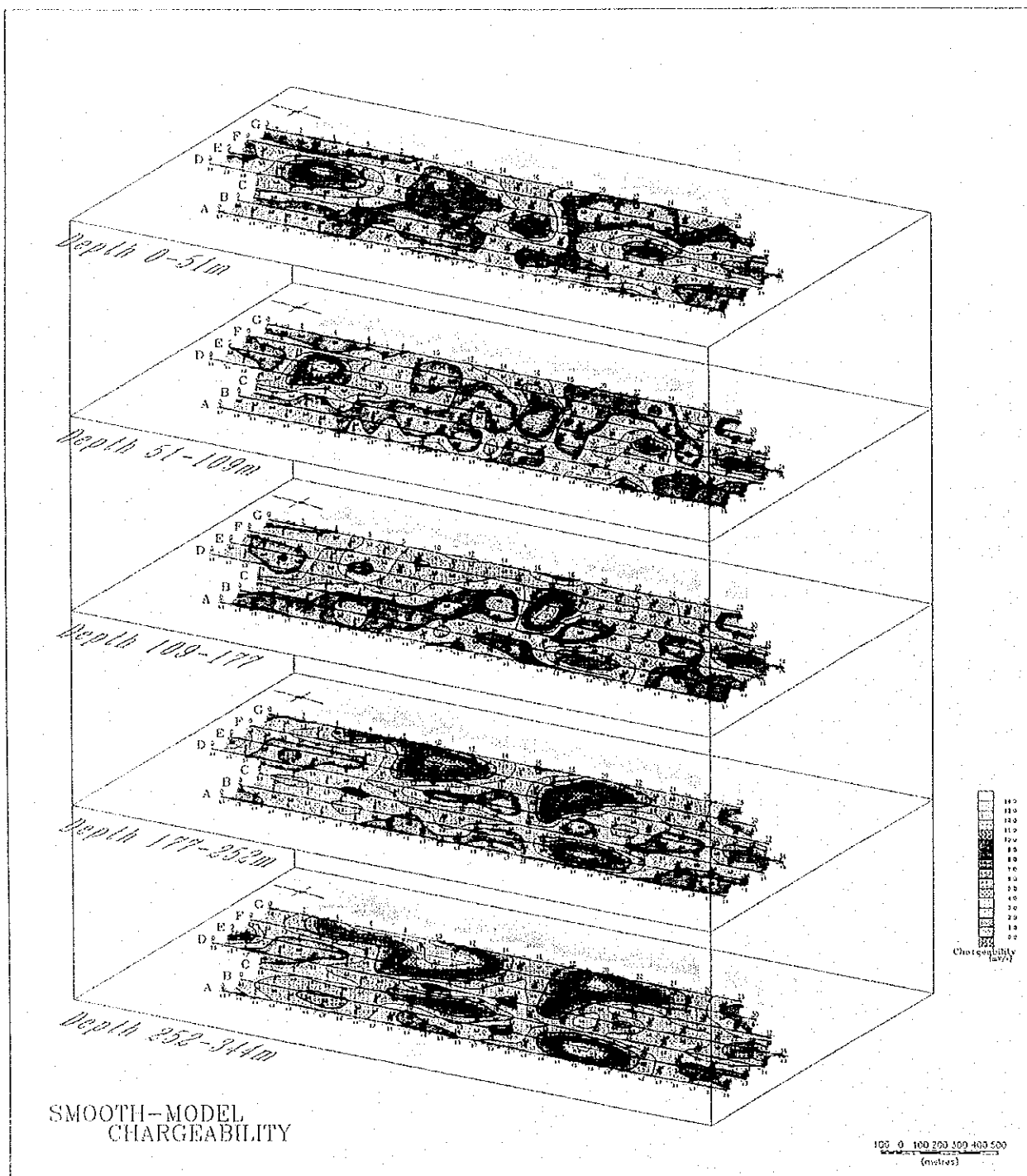


Fig.II-1-19 IP Plane Map of Simulated Result (Chargeability)

METAL FACTOR

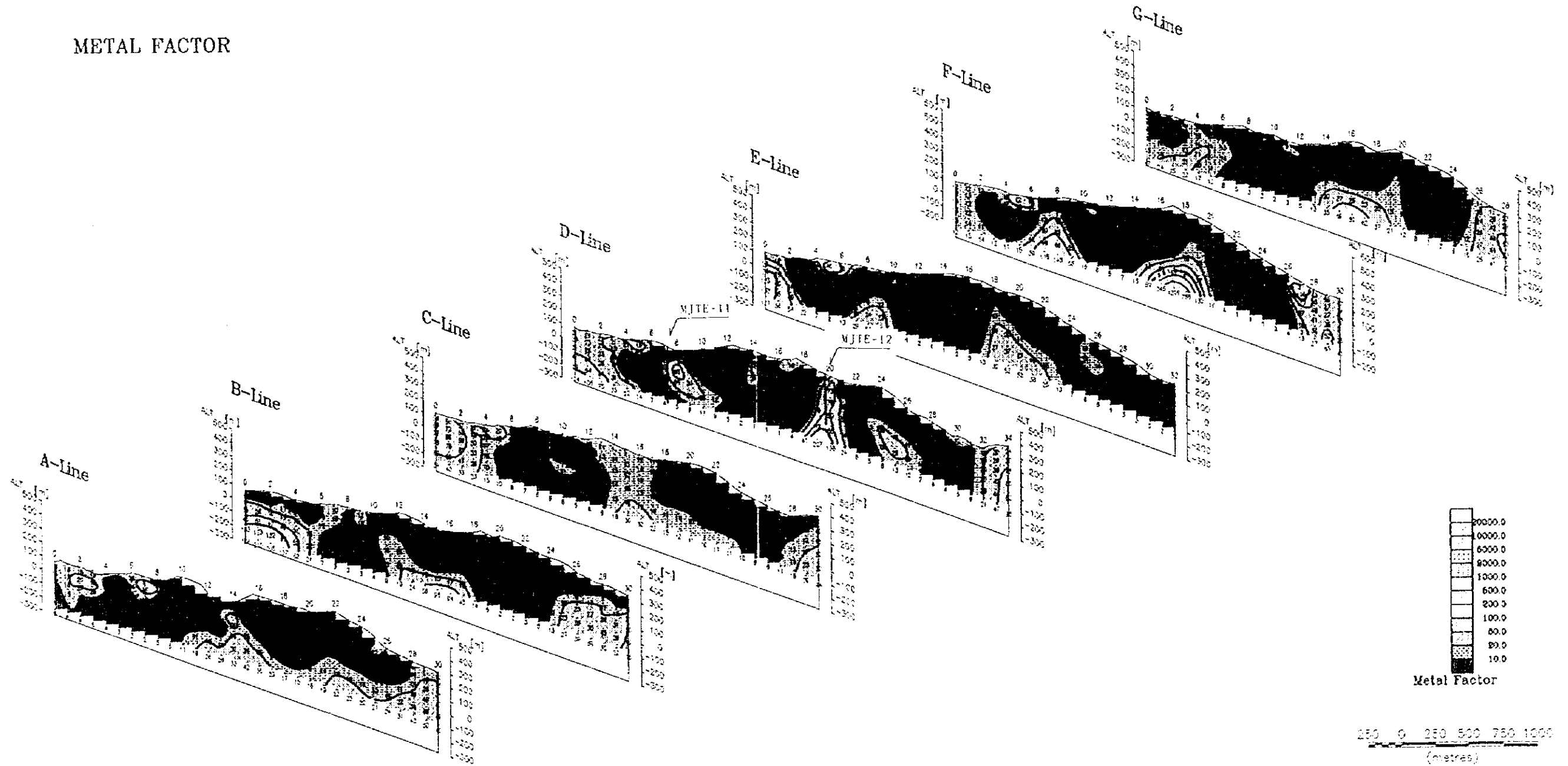


Fig II-1-20 IP Section of Simulated Result (M F)

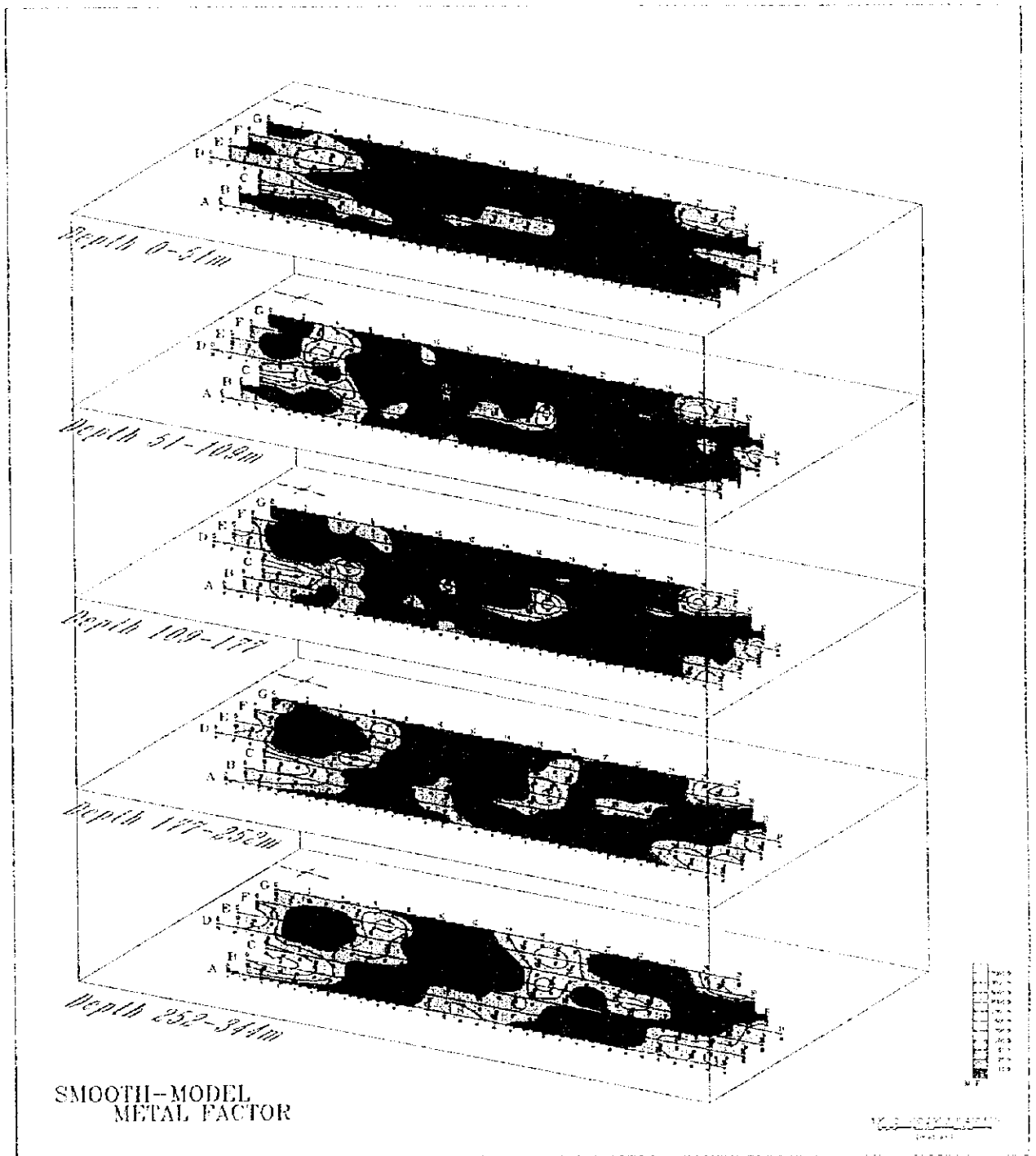


Fig.II-1-21 IP Plane Map of Simulated Result (M F)

LINE-D

RESISTIVITY



OBSERVED

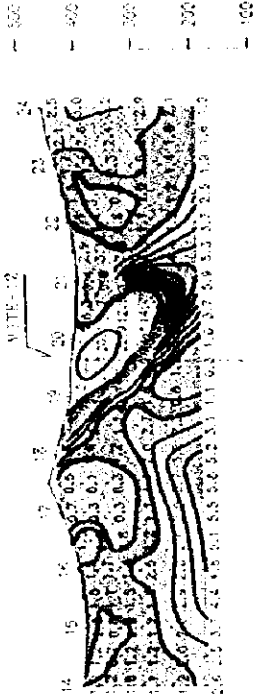
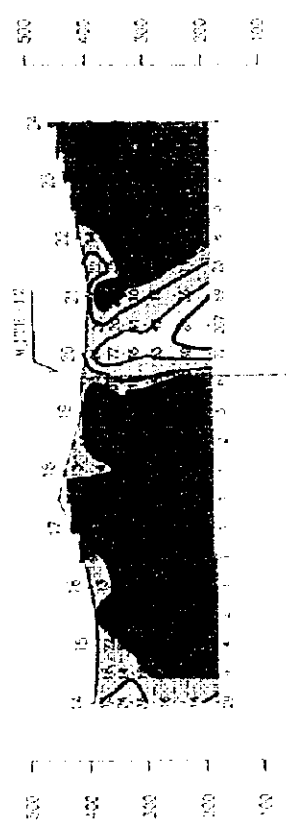


CHARGEABILITY

SMOOTH-MODEL



METAL FACTOR



CHARGEABILITY

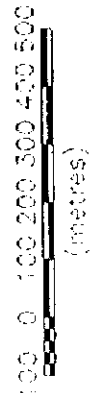


Fig. II-1-22 IP D Section of Simulated Result (a=100m)

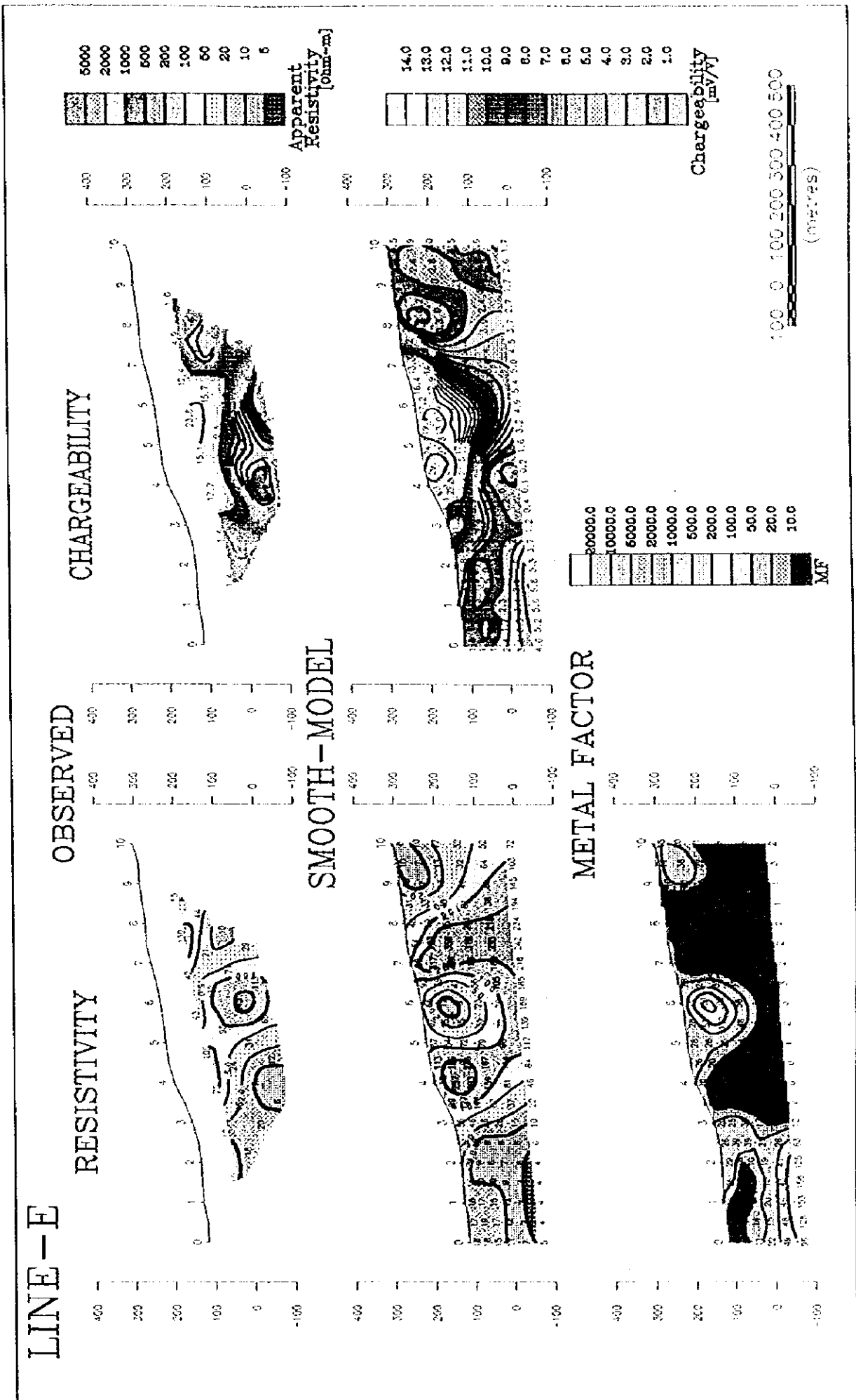


Fig.II-1-23 IP E Section of Simulated Result (a=100m)

Table II-1-6 Results of Analysis (IP Method)

Measuring Line	Site No.	Result of Analysis
A	Nos. 8-16 Nos. 2-8, 14	No anomaly reflecting no mineralization. Shallow level: Mainly hard and massive hematite dacite. Shallow to deep level: Clay rich tuff. MF40 at a maximum
B	Nos. 18-24	No anomaly reflecting no mineralization. Hematite dacite continues to deep level. MF: 40 at a maximum.
C		No anomaly reflecting no mineralization. Mostly low less than $30 \Omega \cdot m$ MF: 40 at a maximum.
D	Nos. 8-12 Nos. 20-24 Nos. 6-8,19	In general, resistivity varies in a short interval. Deep level: High resistivity and high chargeability. Shallow level: High resistivity and high chargeability (hematitic dacite). Vicinity of Karaerik and Karılar ore deposits: Weak anomaly of chargeability. MF: 65 at near depth of 150m in site No. 8 MF:90 at a maximum at depth of 50m or more in site No. 20.
E	Nos. 4-6 No. 19	Low resistivity and high chargeability near Karaelik deposit. High resistivity and weak anomaly of chargeability in the eastward extension of Karılar deposit. MF: 100 at a maximum at depth of about 50m near Karaerik ore deposit.
F	Nos. 8-18 Nos. 22-24 No. 27	In general, high chargeability/high resistivity There is the possibility that the high resistivity zone of $100 \Omega \cdot m$ or more ranging from shallow level to deep level is a hematite dacite integrally formed with those within measuring lines E and G? Lithofacies of high resistivity of $1,000 \Omega \cdot m$ or more at deep level is not determined. MF: 200 up to depth of 100 m. Weak mineralization of Kızılkaya formation.
G		No anomaly reflecting no mineralization. In general, high resistivity / high chargeability . MF: 40 at a maximum.

1-2 CSAMT Survey

CSAMT Method was adopted to clarify the relationship between the geological structure and mineralization

1-2-1 Survey Method

1. Survey in Detail

Fig.II-1-1 and Fig.II-1-2 indicate the location of survey area and measuring points respectively.

Table II-1-7 Specifications of CSAMT Survey

Method	CSAMT
No. of Measuring points	25points
No. of Frequency	12Frequency (1,2,4,8,16,32,64,128,256,512,1024,2048Hz)
Length of Signal Source	1,500m
Direction of Signal Source	N4 ° E
Length of electric potential	50m

2. Setting of Measurement

Survey points were planned to start from the well known IP Survey Linens or corner of road. Open traverse method was adopted to locate exact length of electric potential. Locations of Transmitter Antenna are shown too in FigII-1-1.

CSAMT Method (Controlled Source Audio Frequency Magneto-telluric Method) is a kind of MT Method. While MT Method is a deep sounding method with natural magnetic field as its signal source, CSAMT method is a MT method using artificial signal source which is often adopted for vertical sounding of the place whose depth is less than 1km.

This survey was performed by letting periodic (harmonic) current in the fields of audio frequency run continuously through a wire of 1.5km long whose both ends were grounded and magnetic field orthogonal to the electric field parallel to the signal source (grounded wire) at measuring points.

Fig.II-1-24 is a conceptual chart of measurement. In measuring electric fields, copper electrodes were used as potential electrodes and electrode spacing was 1,500m. For measuring magnetic fields, induction coil magnetic antenna was used. The distance between the signal source and a measuring point should be three times (3δ) or more as large as the skin depth (δ) where the signal (electromagnetic wave) would become almost the same as plane wave. In the area nearer than this (called "near field") the assumption of the plane wave cannot be made and it is difficult to analyze the data.

Skin depth is the depth to which the electro-magnetic wave entered to homogeneous earth (resistivity: ρ) decays to $1/e$ (approx. 37%), and this depth is used as a standard. Skin depth can be obtained by applying the following formula and approx. 70% to the skin depth is considered as the sounding depth:

$$\delta = 503 \sqrt{\rho / f}$$

δ : Skin Depth (m)

ρ : Resistivity of homogeneous medium ($\Omega \cdot m$)

f : Frequency (Hz)

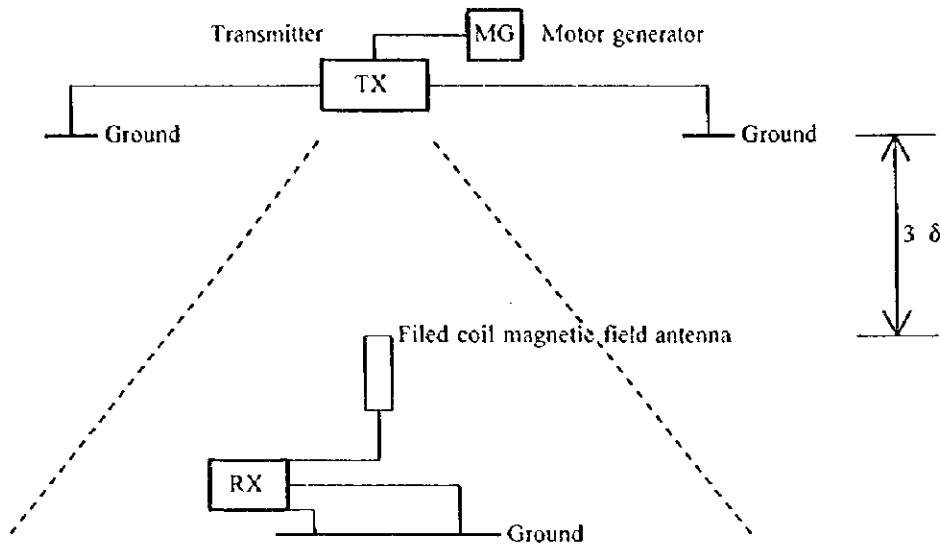


Fig.II-1-24 Measurement Concept of the CSAMT Survey

Table II-1-8 indicates the equipment and materials used for measurement.

Table II-1-8 List of Equipment and Materials

Equipment	Maker	Type	Specification
Transmitter	PHOENIX	LPT-2	max output: 1,000V 15A, 15Kw
Engin Generator	WESTINGHOUSE		max output: 220V 30KW
Receiver	ZONG	GDP-16	16ch. Minimum detectable signal: 0.03 μ V
Transmitter controller	ZONG	XMT-12	Frequency range: 0.001-8kHz
Electrode			Stainless steel
Cable	FUJIKURA		VSF1.25mm ² cable
Measuring compass	USHIKATA		Pocket compass, 100m Esron Ttape
Communication device	KENWOOD	TH-45G	Output 600mAhW

4. Analysis method

1) Data Processing Method

The signals received in electric and magnetic fields are processed in the receiver. By intensity of electric field, intensity of magnetic field, the average of the phase difference between electric fields and magnetic fields and apparent resistivity value are calculated. The formula below which is usually adopted in MT Method was used for calculating apparent resistivity value.

$$\rho = \frac{1}{5 f} \sqrt{E_x/H_y}$$

ρ : Apparent resistivity of earth ($\Omega \cdot m$)

f : Frequency (HZ)

E_x : Electric field (mV/km)

H_y : Magnetic field (γ)

2) 1-D analysis

In order to obtain underground resistivity models, 1-D analysis was made on the assumption that the underground resistivity structure was of a horizontal multi-layered structure. In the analysis, the data which had been obviously under the influence of noise were excluded. Apparent resistivity value was calculated for initial models of each frequency with parameters of the number of layers of horizontal multi-layered structure, thickness of layers and resistivity values. Then simulation technique was used to correct the parameters of the models so that they might become near to the values of actual measurement (the values obtained after near field correction based on the method of Yamashita and Hallof (1985)).

3) 2-D analysis

2-D analysis was conducted using 2-D inversion analysis program of Uchida and Ogawa (1993). In the analysis, the data under the influence of near field were excluded.

1-2-2 Results of the Survey

1. Results of the Survey

Three sections a, b and c were taken in parallel to the signal source so that 2-D analysis is applicable. Measuring points and location of the sections are shown in Fig. II-1-2. General description of each section is given below.

1) Section of Apparent Resistivity (Fig. II-1-25)

Line a

Within the range of high to medium frequencies, low resistivity zone of about $30 \Omega \cdot m$ or less is predominant. In site No.11 of the hematite dacite distribution area, a relatively high

resistivity was observed at high frequencies.

Line b

In the site No.23 of Karaerik deposit, site No.8 of Karılar deposit and site No.22 near Çımaklı, relatively high resistivity (about 60-250 $\Omega \cdot m$) was observed within high to medium frequency range.

Line c

In general, the presence of a low resistivity zone of about 30 $\Omega \cdot m$ or less corresponding to high to medium frequency range was observed.

2) Plane Map of Apparent Resistivity

The pseudoplane map corresponding to the frequencies of 1024, 256, 32 and 8Hz is shown in Fig.II-1-26. A low resistivity zone extends from northwest of the surveyed area to approximately the central part of Topuklu Tepe, located in SE direction.

Site No.23 of Karaerik deposit and site No.8 near Karılar deposit belong to a small-scale high resistivity zone.

2. Results of Analysis

Resistivity structure based on the results of analysis is given only as a broad concept, because the distance between the measuring points by CSAMT is 400m or more.

1) Section of 1-D Resistivity Structure

The resistivity structures determined through the 1-D analysis of the data obtained in various measuring points are arranged in the order of the measuring points and used for making up a 1-D resistivity structure column (Fig.I-1-27). Further, a section of 1-D resistivity structure (panel diagram of Fig.II-1-28) is made up based on the resistivity structures of sections (a,b,c).

Broadly studying all the sections, it can be considered that, in general, the resistivity structure of this area was analyzed as 2 or 3 layered structure, and the resistivity at deep level is high and can be estimated to be about 150 $\Omega \cdot m$ or more.

The resistivity structure at the depth of site No.23 of Karaerik deposit and that at the depth of site No. 8 of Karılar deposit exhibit relatively high value such as about 200 $\Omega \cdot m$ or more.

2) Plane Map of 1-D Resistivity Structure

The resistivity structures at the depths of 100m, 200m, 300m and 400m made into a plane map is rearranged into a panel diagram (Fig. II-1-29).

In general, the low resistivity zone of 50 $\Omega \cdot m$ or less distributes widely reaching near the depth of about 200m. Further, judging from the overall distribution of resistivity, it can be

the depth of about 200m. Further, judging from the overall distribution of resistivity, it can be considered that the E-W-trending low resistivity structure is existing mainly in the vicinity of Karılar ore deposit.

3) Section of 2-D Resistivity Structure

The resistivity structure sections of the lines a, b and c are made up into a panel diagram (Fig. II-1-30).

In general, the resistivity structures are analyzed into 3 layered structure comprising layers of $100 \Omega \cdot m$ or more, $100-50 \Omega \cdot m$ and $50 \Omega \cdot m$ or less.

High resistivity ($100 \Omega \cdot m$ or more) part was calculated in the Karaerik deposit (site No.23) and at a shallow level to a relatively deep level near Karılar deposit (site No.20).

The resistivity structure of $100 \Omega \cdot m$ or more at a deep level was considered to dipping toward in a northwestern direction.

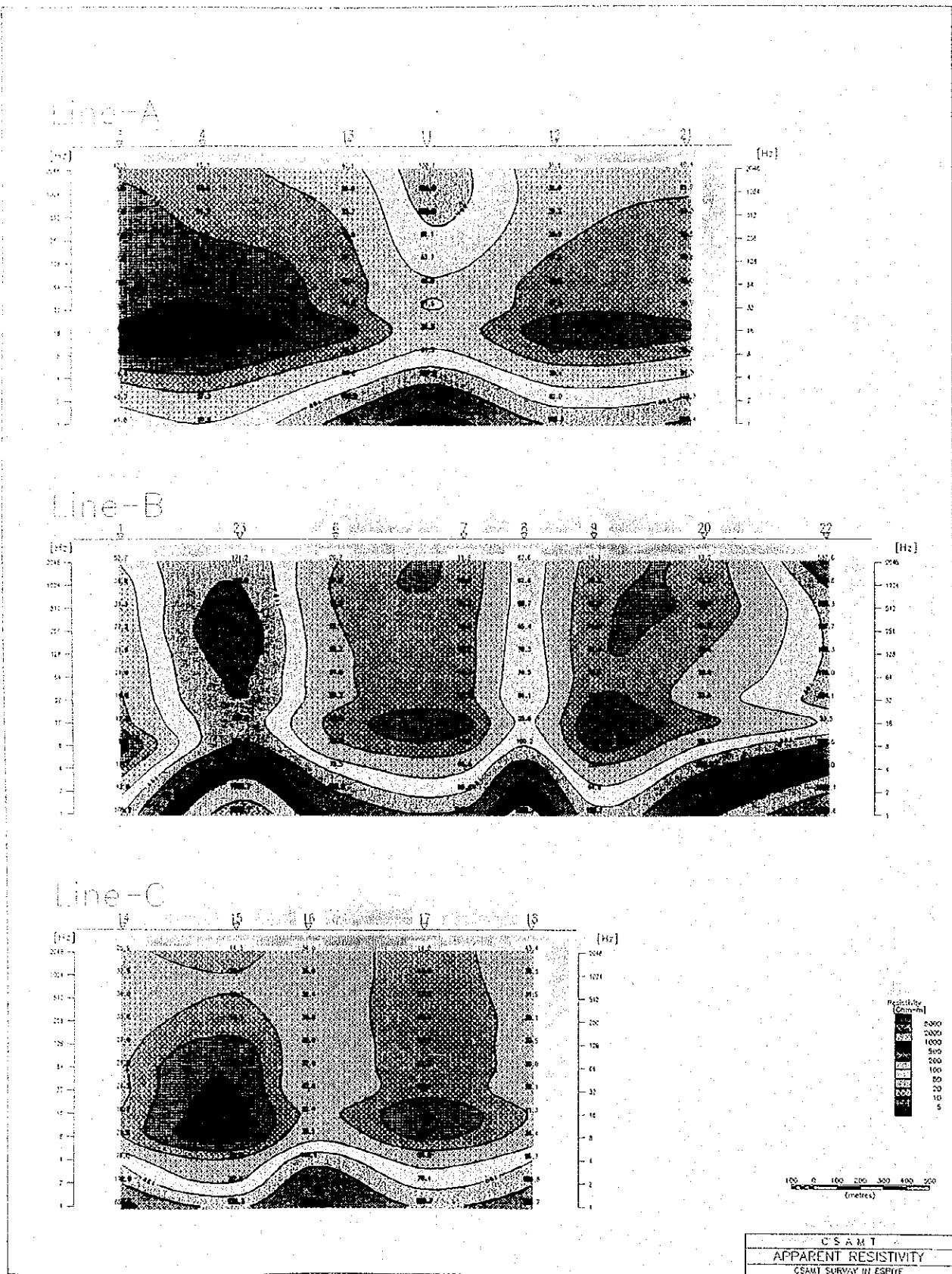


Fig.II-1-25 CSAMT Section of Apparent Resistivity

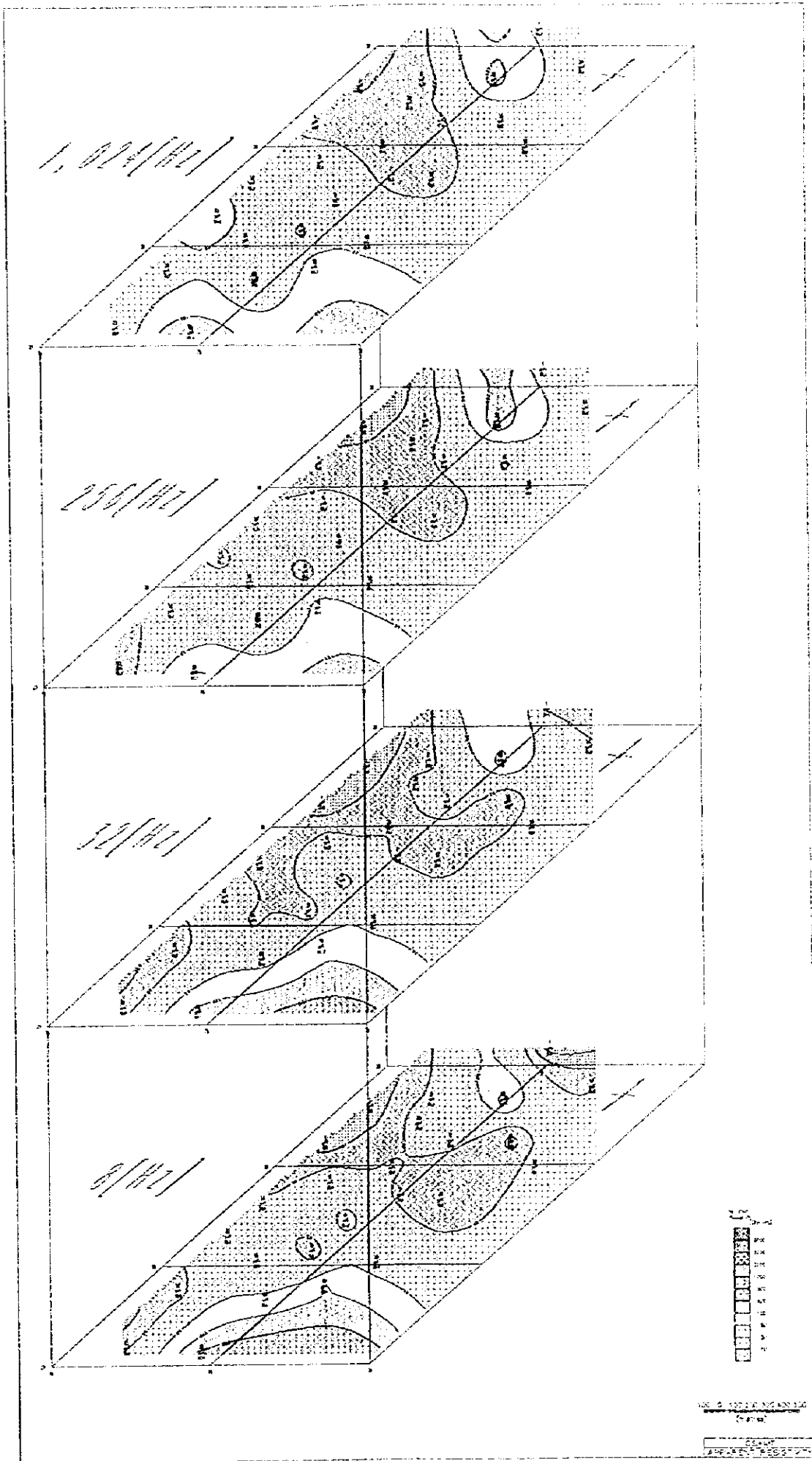
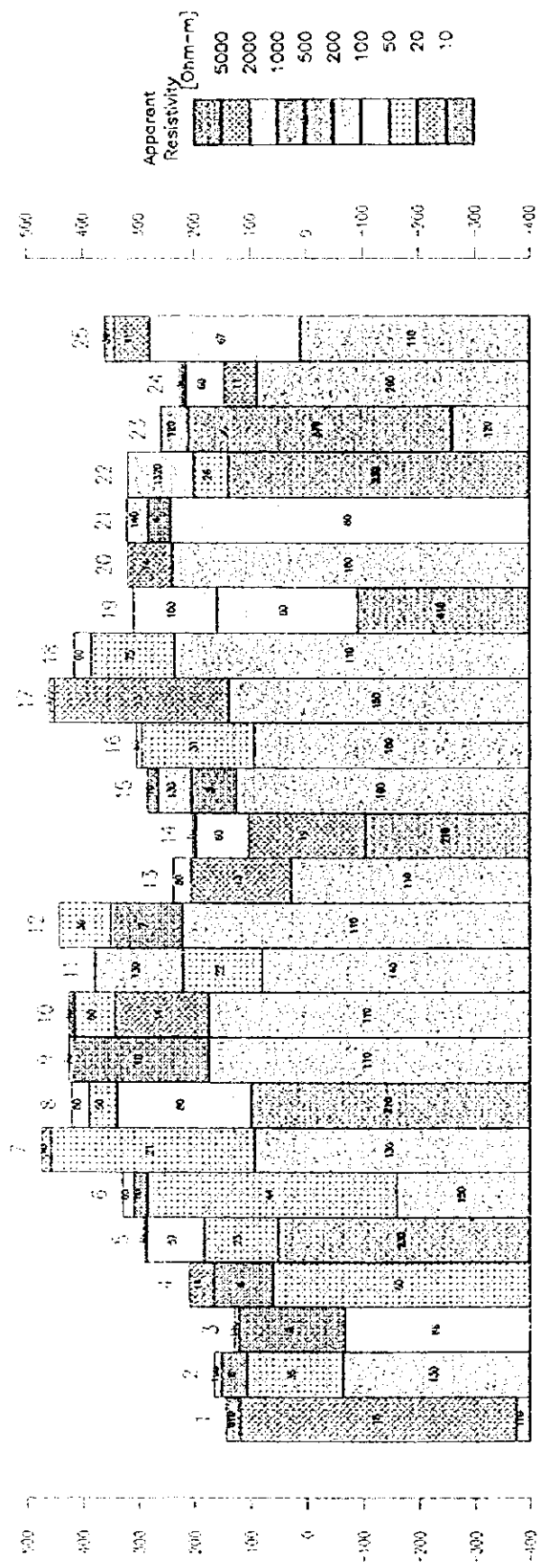


Fig.II-1-26 CSAMT Plane Map of Apparent Resistivity



CSAMT
Resistivity Structure

Fig.II-1-27 CSAMT 1-D Resistivity Structure column

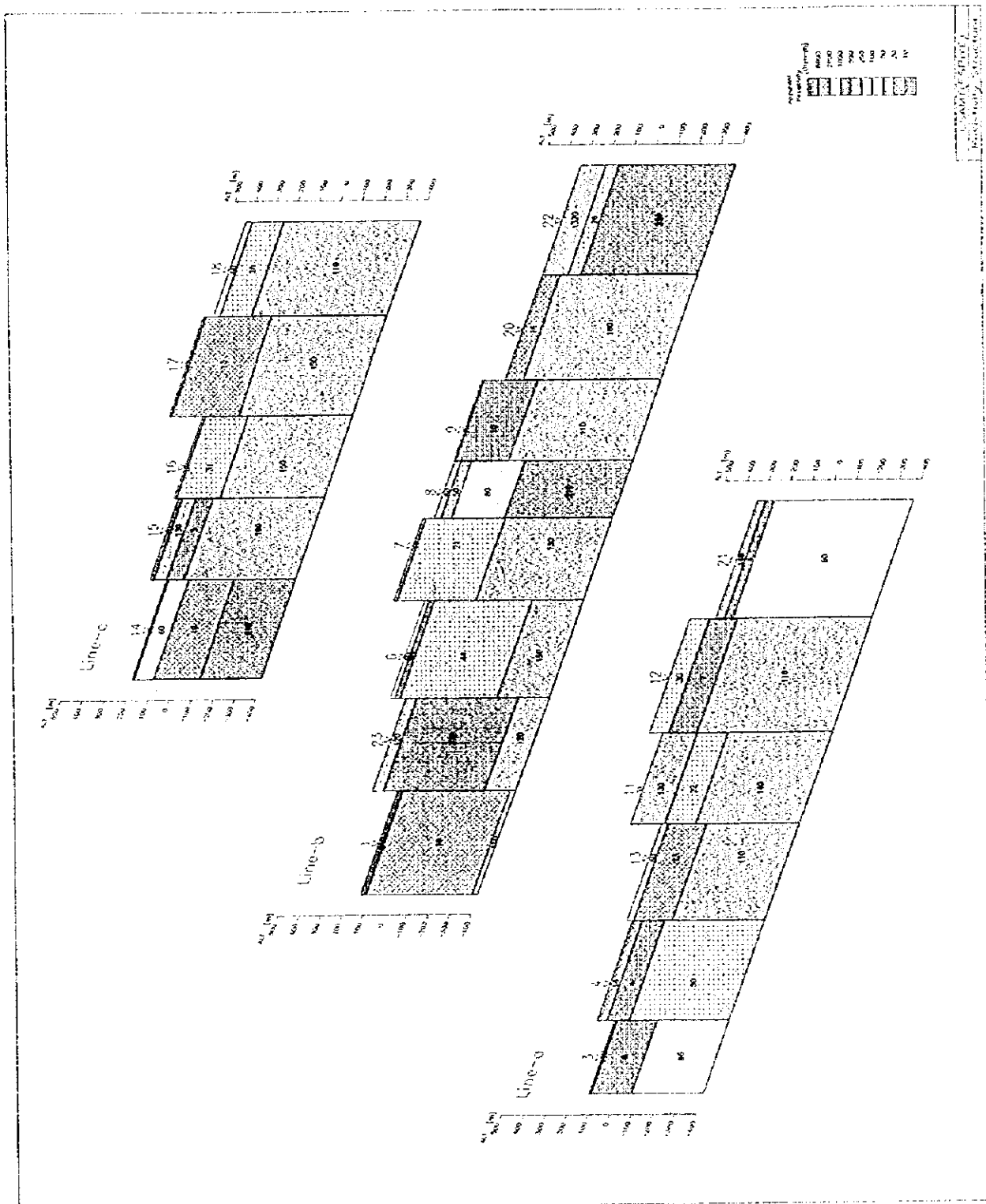


Fig.II-1-28 CSAMT 1-D Section of Resistivity Structure

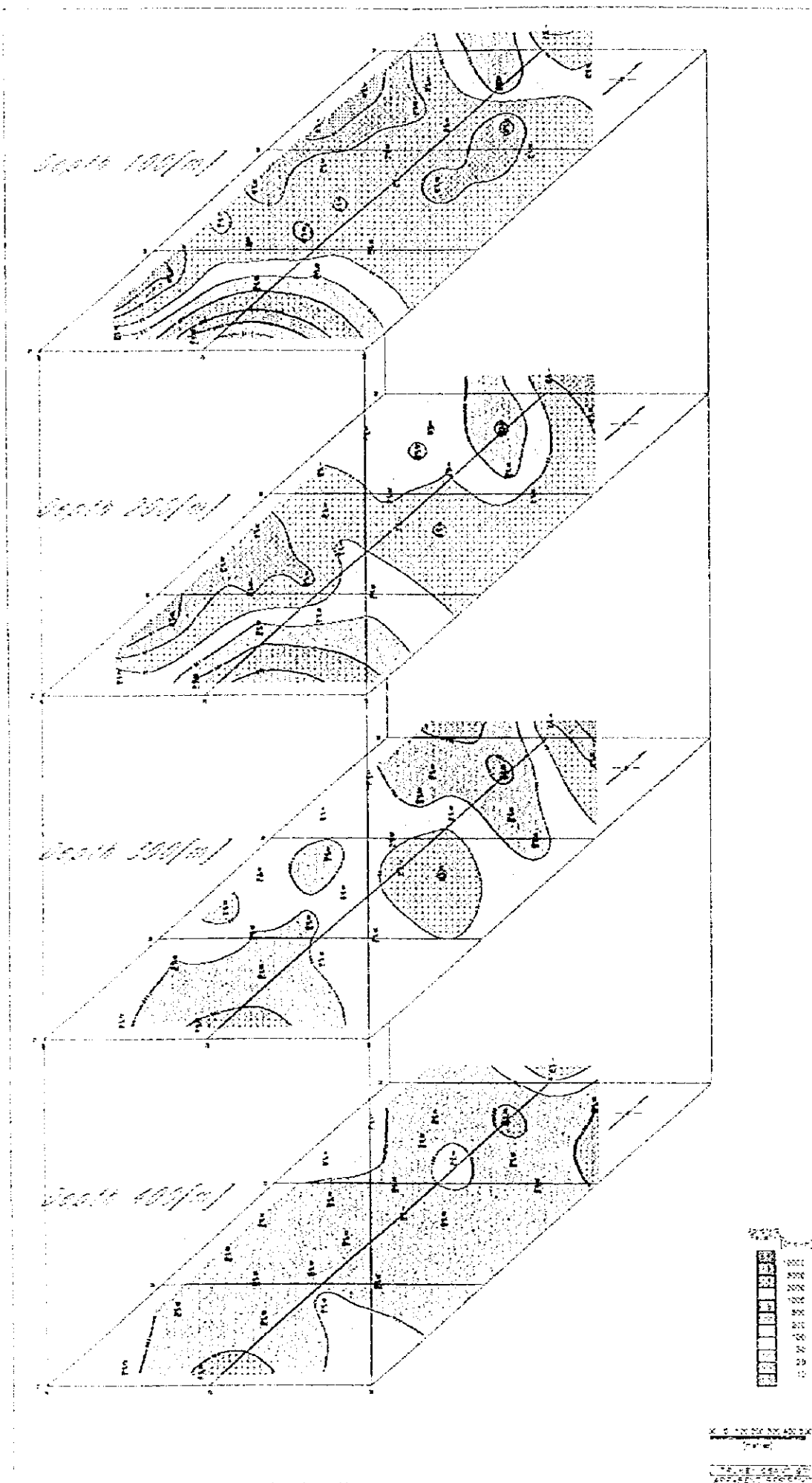


Fig.II-1-29 CSAMT 1-D Plane Map of Resistivity Structure

1-3 Consideration

The results of analyses by IP method and CSAMT method are summarized into a comprehensive analytical map (Fig.II-1-31).

The apparent resistivity in the surveyed area varies from several $\Omega \cdot m$ to 600 $\Omega \cdot m$. The zone covered with hematite dacite shows usually high resistivity (100 $\Omega \cdot m$ or more in general), in this area however, its values are ranging from several $\Omega \cdot m$ to 600 $\Omega \cdot m$. In the hematite dacite distribution area, especially, in a low resistivity zone of several $\Omega \cdot m$, the intense argillization was observed on the surface, indicating that the presence of the fractures and argillization are major factor causing the variation of the resistivity.

In general, the resistivity of other rocks is as low as about 50 $\Omega \cdot m$ or less, mainly caused by the argillic alteration.

According to the results of measurement, the apparent resistivity was within the range of several $\Omega \cdot m$ -600 $\Omega \cdot m$, whereas according to the results of Inversion analysis, the calculated resistivity was within the range of several $\Omega \cdot m$ -about 1,600 $\Omega \cdot m$. A high resistivity zone of about 1,000 $\Omega \cdot m$ or more was analyzed to exist at the depth of 50m or more. Further, according to the result of analysis, in the hematite dacite distribution area, a slightly high chargeability was observed corresponding to the high resistivity zone, this tendency, however being observed throughout the results of the analyses of all the samples.

According to the results of IP survey, the values of chargeability were found to be low in general. Near the Karaerik and Karılar deposits, the weak but obvious anomaly zones were found.

The weak anomaly zones of MF were identified in site No.8 in the line D and near the site No. 29 the line F.

Near the Karaerik and Karılar deposit the distribution form of mineralization was clarified through the measurement by the electrode spacing of 100m.

In terms of analysis, the unit of calculated MF is horizontal distance of about 50-70m, and the unit of thickness is 50m.

According to those values of MF as determined by analysis, when the unit described above was adopted, the value of MF was found to be 100 at a maximum near the old ore deposit. Further, the largest value of MF within the surveyed area was 200 as observed near the site No. 27 in the line F. However, according to the results of the property tests of ore samples in terms of the relationship between the value of MF and the mineralization, the value of MF was about 10 or less where there was no mineralization, about 100-1,000 for siliceous ore, about 2,000 or more for black ore and about 10,000 or more for yellow ore. Judging from these facts, it can be considered that the presence of a weak anomaly of MF suggests the presence of weak mineralization.

According to the results of the resistivity analysis by IP method and the result of 1D analysis by SCAMT method, it can be identified that the low resistivity structure running east-west direction exists at about the center and north of the surveyed area.

Concerning the results of the analysis by the CSAMT method, the distribution of resistivity in neighboring regions are not clear because of insufficient number of measuring points; however, the results of analysis indicates that near the Karaerik deposit and the Karılar deposit, slightly high resistivity was observed even in relatively deep level.

According to the result of 2-dimensional analysis, high resistivity ($100 \Omega \cdot m$ or more) was observed in general at deep levels. The depth of region exhibiting high resistivity is estimated to be about 300-600m, this region being considered gently inclining downward in the northwestern direction of the surveyed area. This tendency coincides with the result of gravity structure.



